

Incoherent Long Wavelength Detectors

At microwave and radio frequencies, the photon energy is $<1\text{meV}$ corresponding to sub-K temperatures.

Bolometers : germanium thermistors of low thermal inertia, heat up on absorption of radiation.

Individual devices coupled with waveguides to telescope.

Operated at mK temperatures but even then may not be background-limited

Labour intensive production – limited pixel numbers, individual wiring and read-out

SCUBA individual pixel



SCUBA focal plane

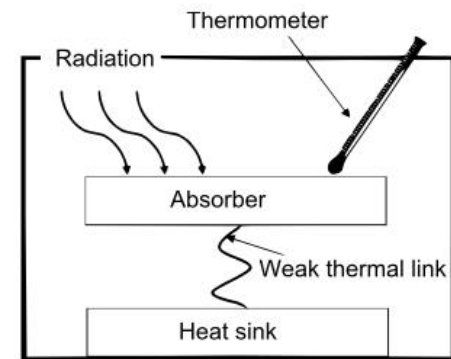
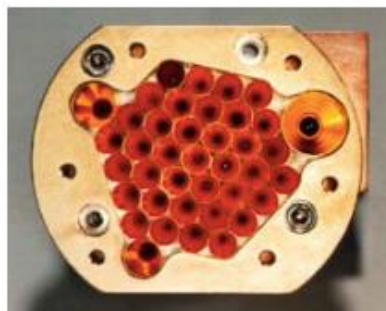


Figure 1: Schematic of a bolometer. Radiation is absorbed in the absorber. A thermometer detects the resulting increase in temperature. Heat is removed by a weak thermal link to a heat sink.

Array Detectors : TES

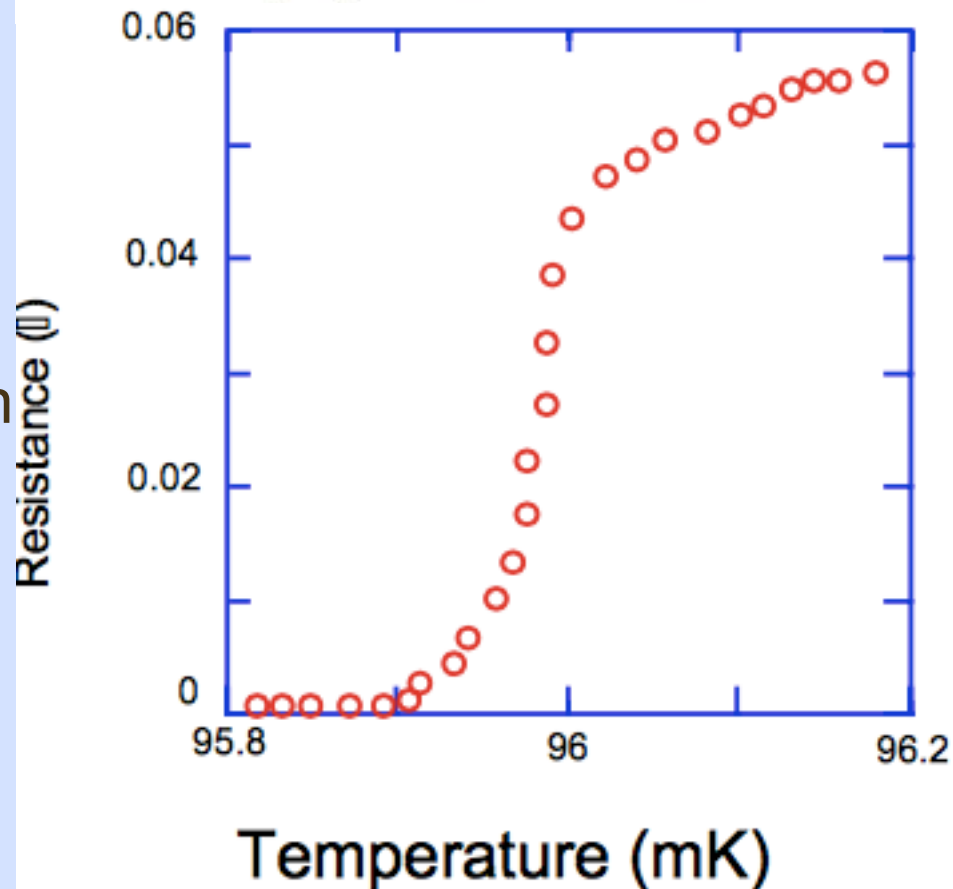
Transition edge sensor devices exploit the super-conducting transition to give high sensitivity (large dR/dT)

TES arrays are bump-bonded to a multiplexor allowing large format arrays

Operated at $\sim 60\text{mK}$, with bias level control to keep on transition

Instrument cooled below 10K to reduce background

SCUBA-2 maps the sky at 450 and $850\mu\text{m}$ with 4 arrays each with 1280 TES pixels in each waveband.



(A Woodcraft 2006)

Kinetic Induction Devices

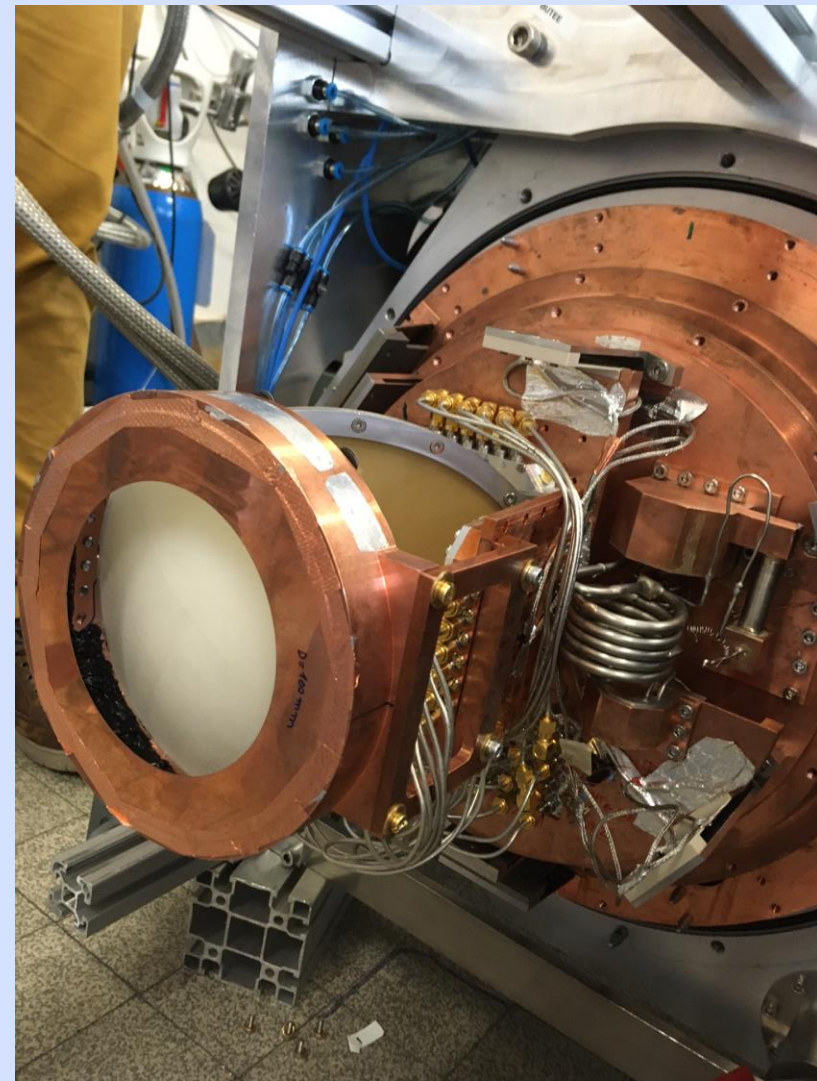
KIDS use superconductor *below* the transition temperature

Radiation breaks Cooper pairs which act rather like electron-hole pair creation in semiconductor, but with smaller energy gap

Signal detection is via the change in AC inductance, which should lead to simpler detector

fabrication and signal processing

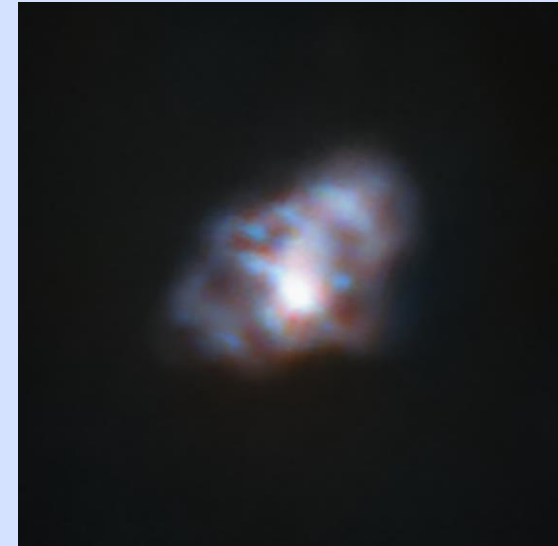
Instrument will still need to be cooled below 10K, and the detectors to be maintained near 50mK



Concerto instrument mounted on APEX. Operates at 120-300 GHz with 2 x 2152 pixels

Kinetic Induction devices

- Promising technology for large format, microwave detector arrays
- Pixels can provide low energy-resolving imaging systems
- Potential at other wavelengths, including Near-IR/visible



Crab nebula imaged with Concerto



NGC6334 imaged with Concerto

Coherent Detector Systems

- Single or few pixel receivers sensitive to both intensity and phase are used for spectroscopy or in interferometers
- At high frequencies, generally Superconductor-Insulator-Superconductor (SIS) devices The incoming electromagnetic wave can excite a charge carrier sufficiently for quantum tunneling across the bandgap to occur.

ALMA operates at frequencies too high for direct amplification. Mixing with a stable wave from a Local Oscillator gives a beat pattern that can be processed

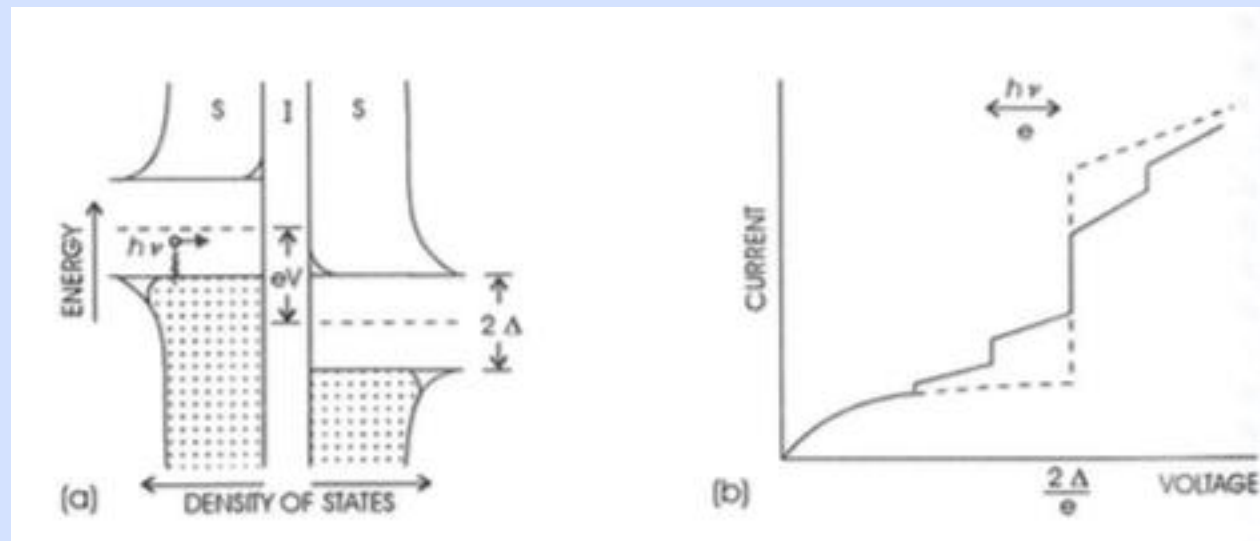
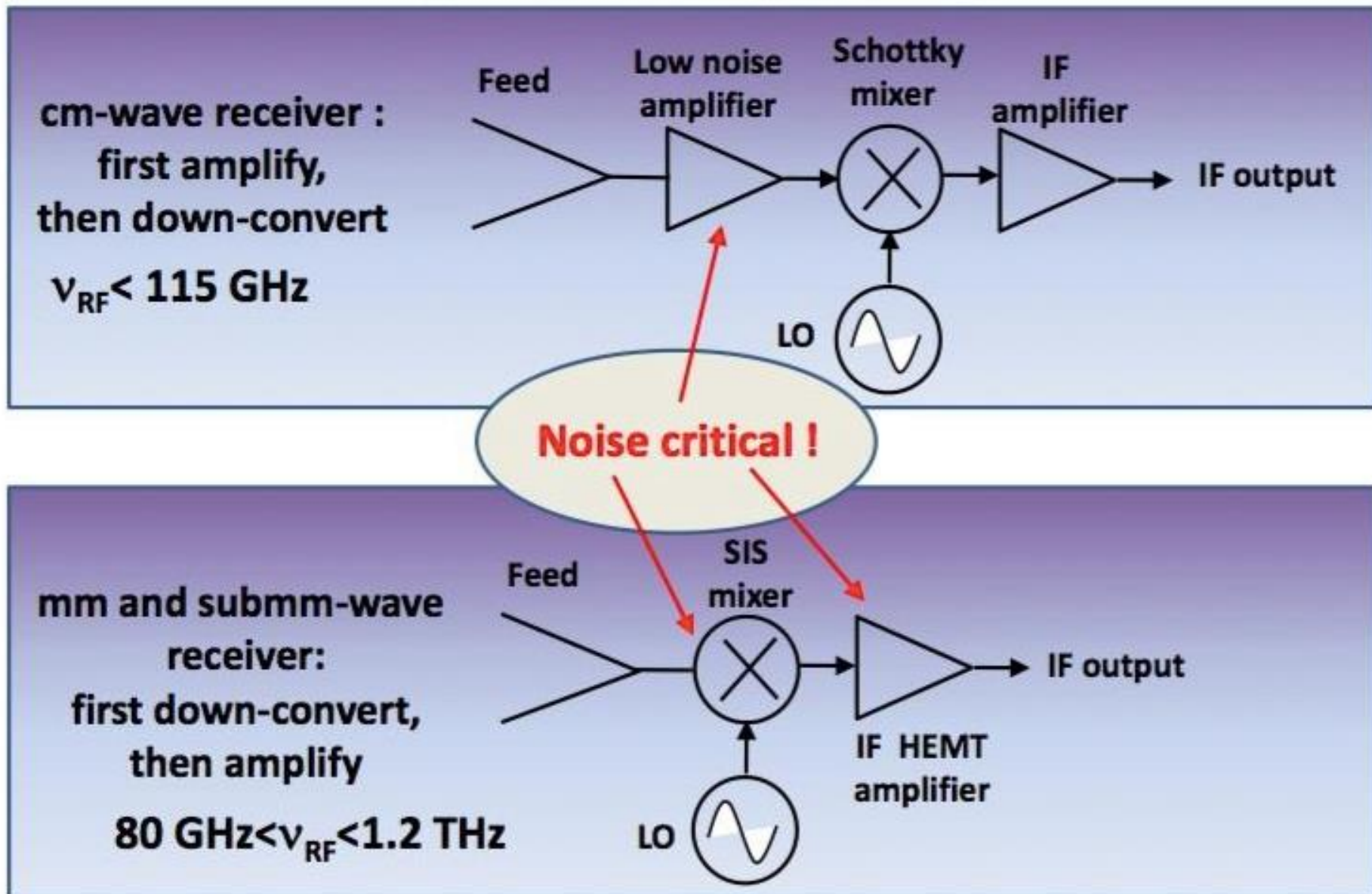


Fig. 12.15. (a) shows the basic structure of the energy levels in an SIS detector. No current flows if $eV < 2\Delta$. Absorption of a photon can excite a charge carrier to the energy where the tunnel effect occurs; (b) shows the current-voltage behaviour without illumination (solid line) and with photons present (dashed line).

Synoptic diagram of heterodyne receivers (basic building blocks)



Heterodyne Signal Processing

At high frequencies, need a multi-stage process: e.g

- ALMA Band 9 (602-720 GHz) is mixed with a stable oscillation between 610-712 GHz to give an IF between 4-12GHz.
- This Intermediate Frequency is passed to a second mixing stage with LO2 ~4-10GHz to give IF(2) ~ 0-2GHz which can be transmitted to the correlator

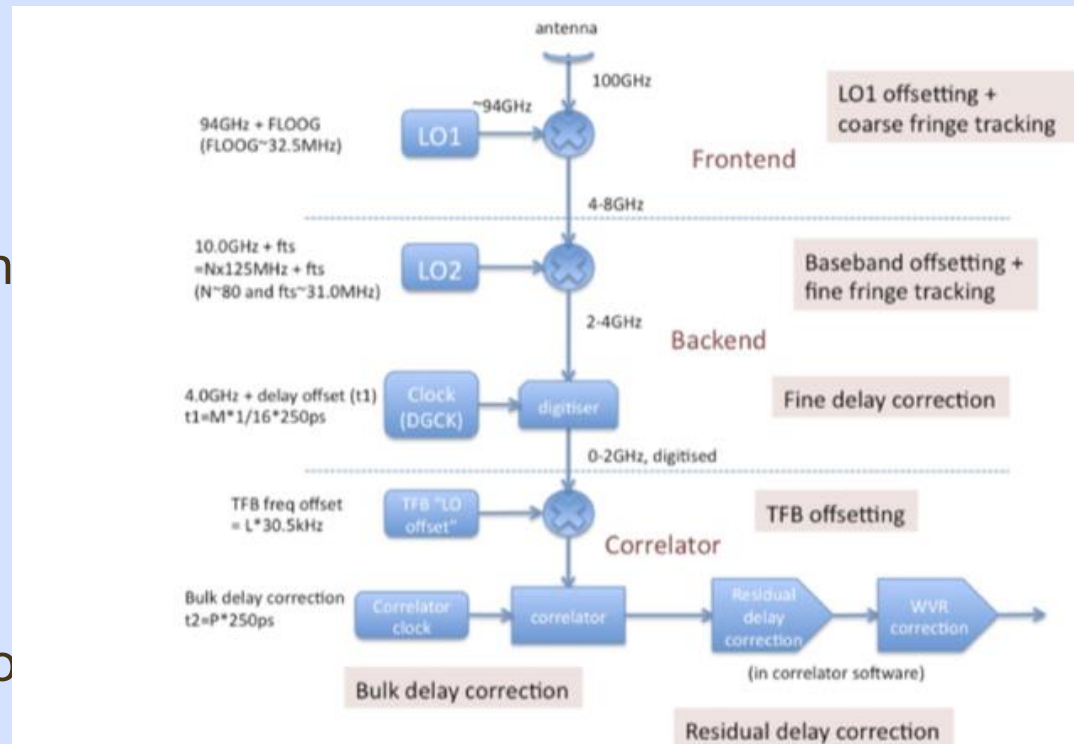


Figure B.1: Overview of ALMA frequency downconversion, LO mixing and delay corrections. This takes place in the Frontend, Backend, and Correlator. Example frequencies are given for an observation at a sky frequency of 100 GHz seen in the USB. Some LOs (e.g. LO1) are continuously tunable; others have quantized tuning steps, such as LO2 (which can be changed in a multiple (“N”) of 125 MHz plus an finely-adjustable offset of “fts”), the TFB LO (which uses a multiple “L” of 30.5 kHz) and the Bulk Delay Correction (which has steps of 250 ps.

TFB Tunable Filter Bank

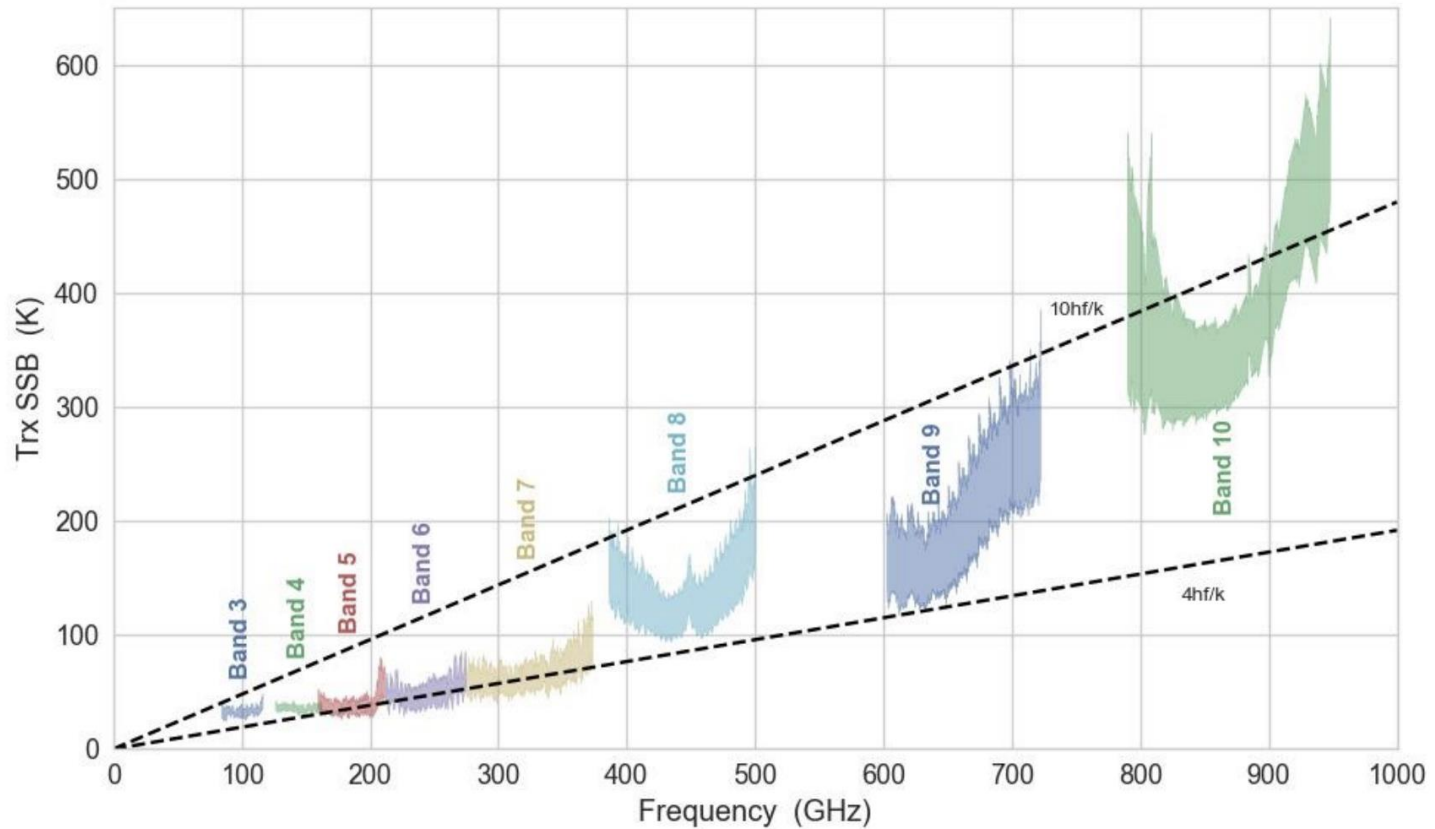


Figure 1: Receiver noise temperature for the ALMA receiver, where the shaded region encompasses 75% of the receivers about the median receiver temperature. Bands 3-8 are 2SB receivers, and Bands 9 and 10 are DSB. The noise temperature shown for the DSB receivers are twice the DSB temperatures. Band 1, which is under construction, has a receiver specification of < 25 K across 80% of the band.

- Noise temperatures for the ALMA Receiver Bands plotted against receiver frequency on the horizontal axis. The low frequency receiver bands 4 – 7 have a performance within a factor 4 of the quantum limit. Gains can come from wider bandwidths or efficiency improvements, especially low-noise, wide-band amplifiers.
- Band 1 (35 – 50 GHz) are being deployed and Band 2 receivers are in production.

Other Detectors and Developments

- Photomultiplier tubes – used in CTA
 - Fast response, blue/UV sensitivity
- Avalanche photo-diodes (APDs)
 - High sensitivity, low noise, useful for Wavefront Sensors and fringe tracking
 - HgCdTe APDs from Selex have demonstrated sub-electron read noise (G Finger et al 2012)
- Detector developments:
 - CCDs & IR hybrids :Larger formats, better uniformity, lower noise
 - CMOS developments
- Microwave & Radio : wider bandwidths, lower noise

References

- Basic Image Processing and CCD features :
- <https://www.eso.org/~ohainaut/ccd/>
- Starlink CCD Data Reduction Cookbook :
- <http://www.starlink.ac.uk/docs/sc5.htx/sc5.html>
- “Infrared Detector Arrays for Astronomy” - G.H. Reike, Annual Review of Astronomy and Astrophysics, 2007
- ALMA Technical Handbook
- <https://almascience.eso.org/documents-and-tools/cycle9/alma-technical-handbook>

Imaging and Photometry

Brightness



- Probably the most fundamental property of any astronomical object is its energy output
 - Provides information on energy source and scale
- By measuring the brightness of an object, we can calculate the energy output
 - Providing we know how far away it
 - and we correct it for any energy loss
 - providing the output is isotropic
 - and we can measure the total brightness, i.e. across the full spectrum (and account for any other energy loss such as neutrinos)
 - Or for known object classes, accurate photometry may indicate distances
- To do this accurately, we have to calibrate our measurements carefully and turn them into useful numbers – and that is where the trouble starts.....
- Unfortunately different wavebands use different measures of brightness

Magnitudes

- Historic brightness scale :
 - mag 1 is bright and 6 is the faintest visible to the eye
 - brightest star at V: Sirius has $m_V = -1.4$,
 - HST limit is $\sim 31^{\text{st}}$ magnitude, $\sim 10^{13}$ times fainter than Sirius
- Logarithmic scale, 5 mag \equiv factor of 100
 - proposed by Norman Pogson of the Radcliffe Observatory (1856)
- Standard photometric systems based on photoelectric measurements made in the 1960s (Johnson - UBVRI):
 - U is shortward of Balmer discontinuity
 - B is peak of photographic plate response
 - V is peak of human eye response
- Vega (Spectral type A0, $T \sim 10^4 \text{K}$) had mag=0 in all bands
- Other stars are then measured with respect to this star – fundamental calibrator

Types of Magnitude

- *Apparent* - m - measured magnitude relative to Vega or other fundamental calibrators in a defined passband, e.g. m_V
- *Absolute* - M - the apparent magnitude the object would have if it were at a distance of 10pc. So a measure of the total output within the band
- *Bolometric* - M_{bol} is the bolometric magnitude of the star given by
$$M_{\text{bol}} = -2.5 \text{ Log}_{10} (L_*/L_0)$$
 L_* (the star's luminosity in Watts) is relative to an object with a luminosity of $L_0 = 3.0128 \times 10^{28}$ W across the whole electromagnetic spectrum (the IAU-decreed luminosity for $M_{\text{bol}} = 0.0$)
- The bolometric magnitude of the sun is $M_{\text{bol}} = 4.74$
- Note $M_{\text{bol}} = M_V - \text{BC}$ - the Bolometric Correction which accounts for the emission outside the V passband
- In practice, may also need to account for interstellar extinction (A_V) so that $M_{\text{bol}} = M_V - \text{BC} - A(V)$

Distance Modulus

A measure of the distance expressed as the difference between the apparent magnitude of object compared to what it would be at a distance of 10pc : $\mu = m - M$

$$\text{Log}_{10} (d) = 1 + \mu / 5, \quad \text{with } d \text{ in pc}$$

$$(m - M)_V = 5 \times \log (D/10\text{pc})$$

e.g. the distance modulus to the LMC (50kpc) = 18.5



Vega magnitudes work well for stellar photometry as the colours from pairs of filters indicate stellar temperatures

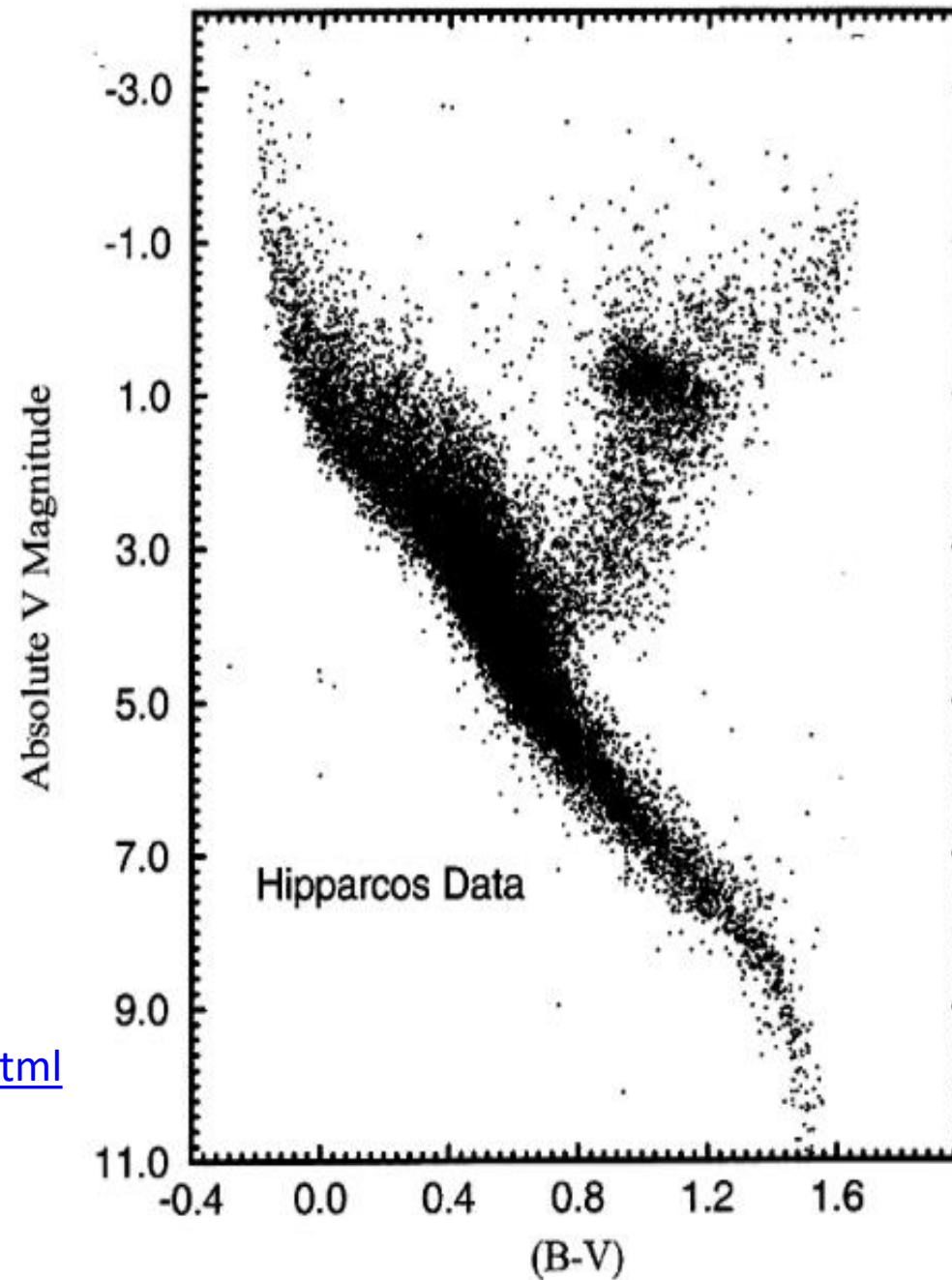
Different Photometric systems use different filters; e.g. **Stromgren** (narrow band filters used to estimate T, g, metallicity)

AB magnitudes :

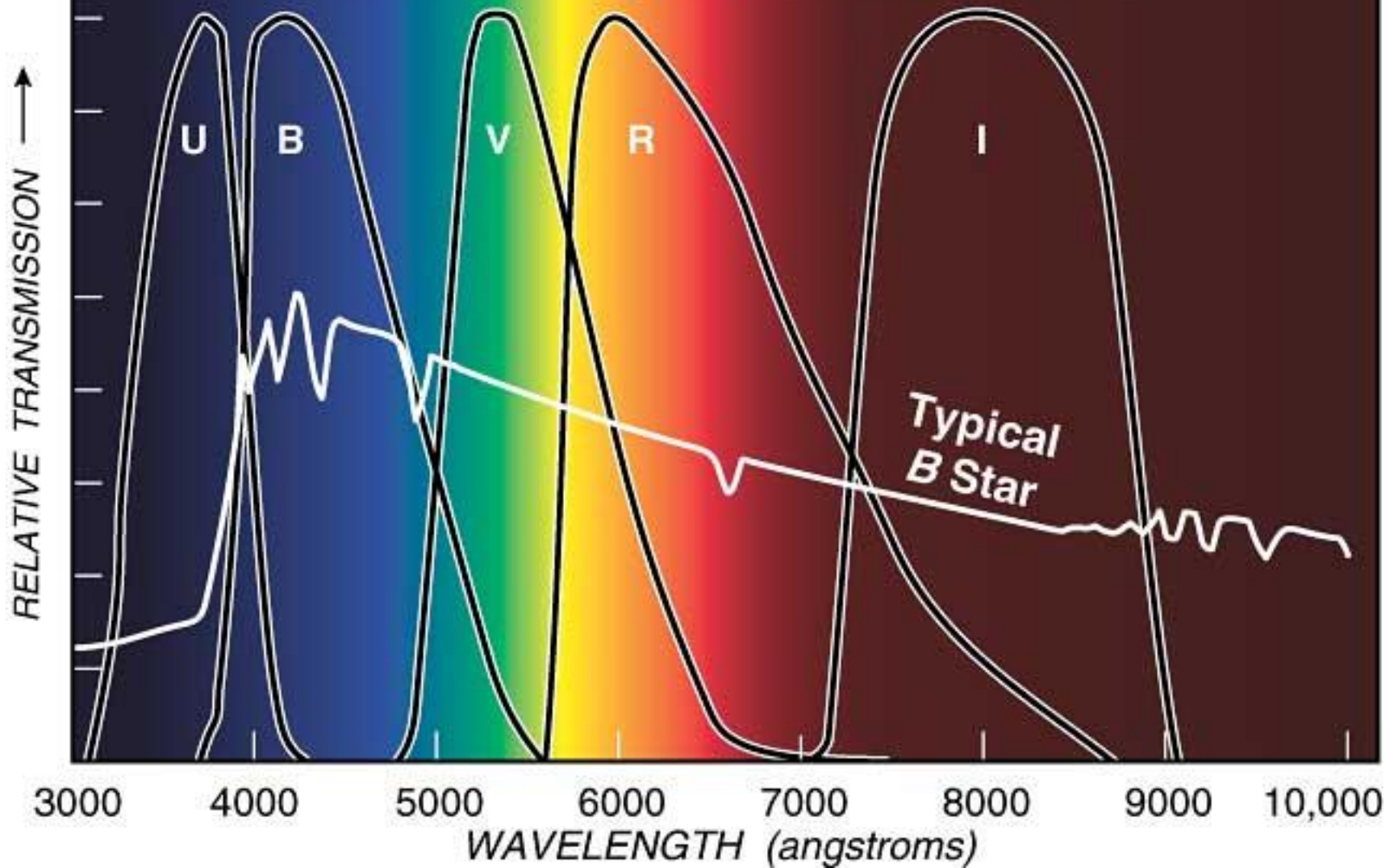
Source with constant flux per unit freq. has zero colour. With flux measured in $\text{erg s}^{-1} \text{cm}^{-2} \text{Hz}^{-1}$
 $m_{\text{AB}} = -2.5 \log(f) - 48.60$

Sloan u'g'r'i'z' system similar to AB
<http://classic.sdss.org/dr4/algorithms/fluxcal.html>

STMAG (Space Telescope magnitude system) Source with constant flux per unit wavelength has zero colour

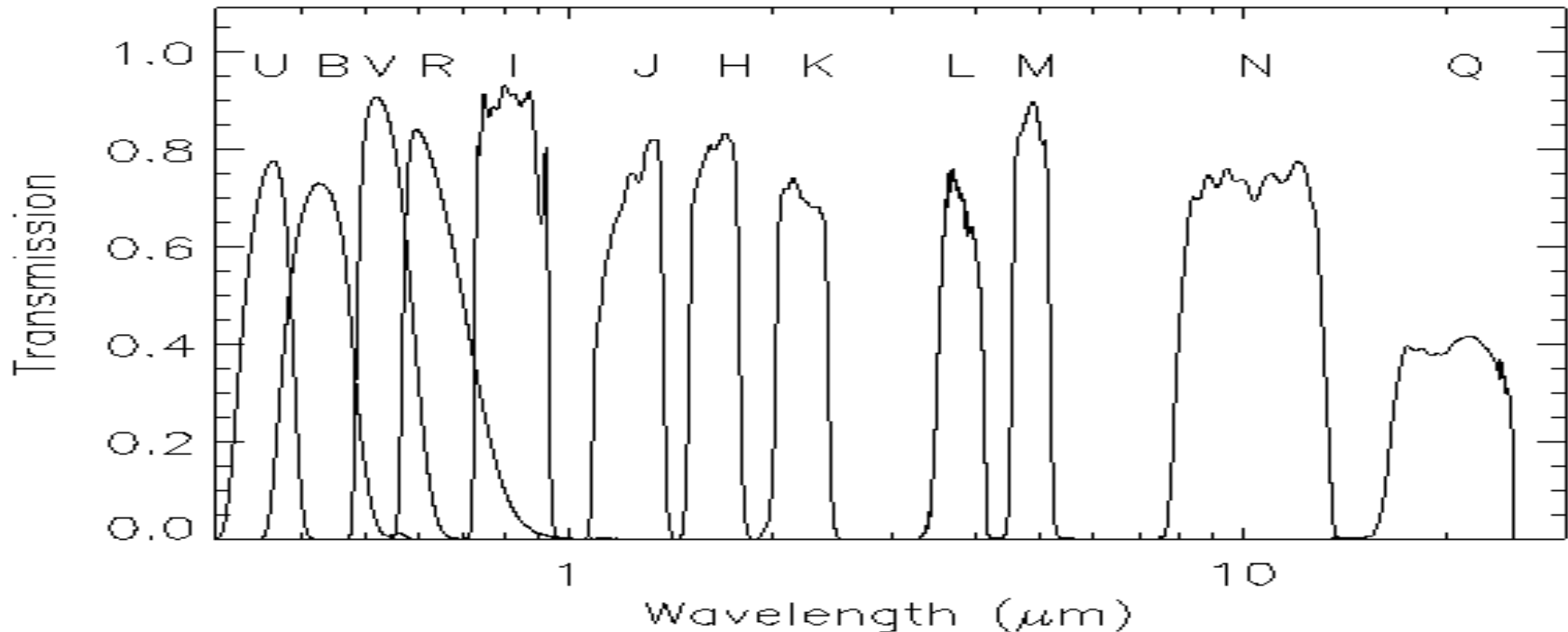


Standard Photometric Filters

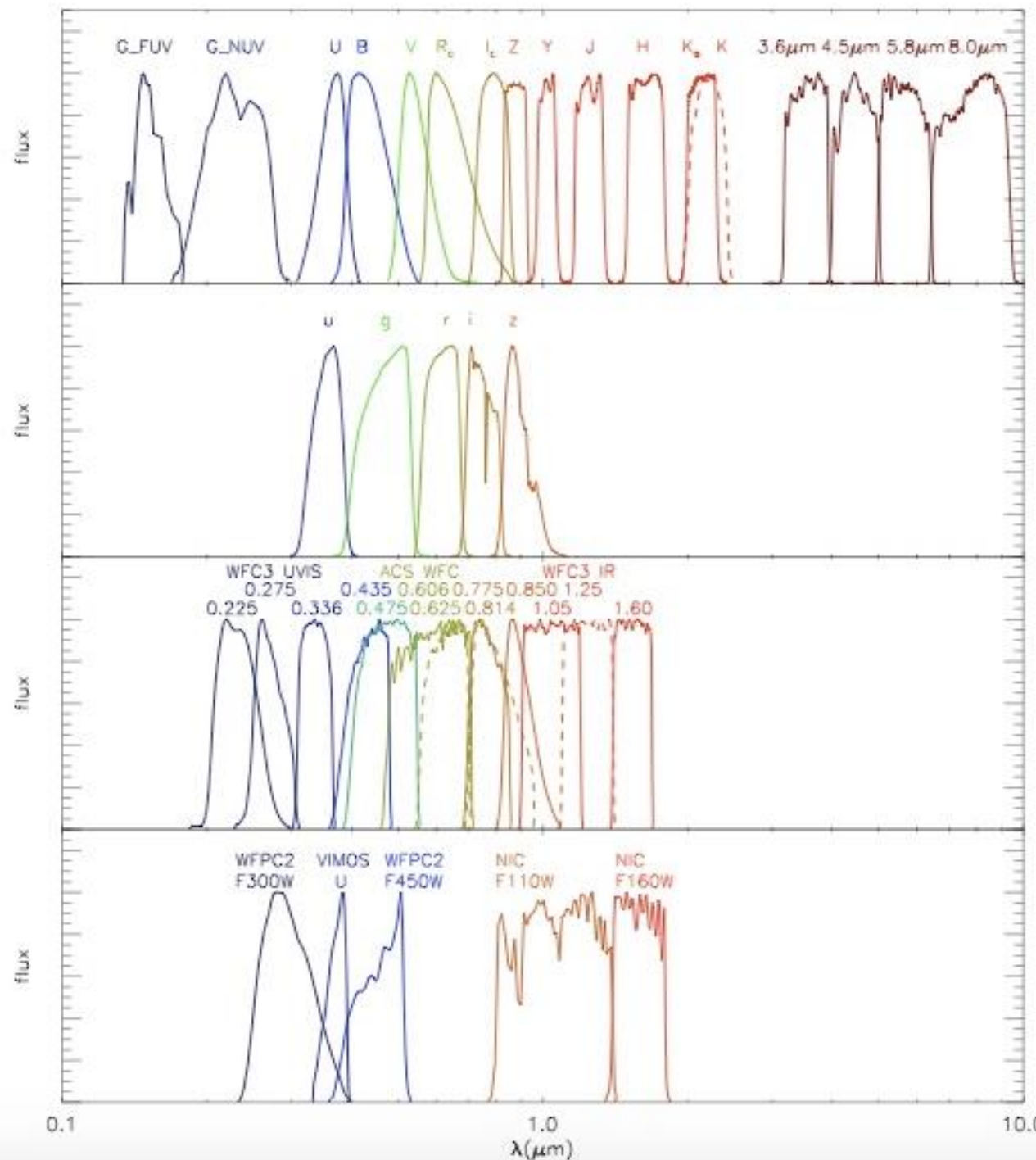


Extension to IR

- UBVRIJHKLMNQ 0.3 to 25 μm
 - Additional filters : Z \sim 0.88 μm , Y \sim 1.02 μm
 - IR filters match the atmospheric windows for ground-based observations.
 - Satellites have more options



- Comparison of different filter profiles:
- Top GALEX FUV and NUV, Johnson-Bessel U, B, V, Cousins R_c , I_c , VISTA Z, Y, J, H, K_s , Johnson-Bessel K and IRAC 3.6 μm , 4.5 μm , 5.8 μm and 8.0 μm bands;
- Second panel: SDSS u, g, r, i, z bands;
- Third panel: bands from HST instruments, three UV bands from the WFC3-UVIS (0.225 μm , 0.275 μm , 0.336 μm), seven optical bands from the ACS-WFC (0.435 μm , 0.475 μm , 0.606 μm , 0.625 μm , 0.775 μm , 0.814 μm , 0.850 μm) and three near-infrared bands from the WFC3-IR (1.05 μm , 1.25 μm , 1.60 μm);
- Bottom panel: VIMOS U band, 2 NICMOS near-infrared bands (1.1 μm and 1.6 μm) and two WFPC2 bands (0.30 μm and 0.45 μm).



Magnitudes and fluxes

Vega Flux Zeropoints

Quantity	U	B	V	R	I	J	H	K	Notes and units
λ_{eff}	0.36	0.438	0.545	0.641	0.798	1.22	1.63	2.19	microns
$\Delta\lambda$	0.06	0.09	0.085	0.15	0.15	0.26	0.29	0.41	microns, UBVRI from Bessell (1990), JHK from AQ
f_{ν}	1.79	4.063	3.636	3.064	2.416	1.589	1.021	0.64	$\times 10^{-20}$ erg cm ⁻² s ⁻¹ Hz ⁻¹ , from Bessell et al. (1998)
f_{λ}	417.5	632	363.1	217.7	112.6	31.47	11.38	3.961	$\times 10^{-11}$ erg cm ⁻² s ⁻¹ A ⁻¹ , from Bessell et al. (1998)
Φ_{λ}	756.1	1392.6	995.5	702.0	452.0	193.1	93.3	43.6	photons cm ⁻² s ⁻¹ A ⁻¹ , calculated from above quantities

These are for the Vega magnitude system and the Bessell et al. (1998) Johnson-Cousins-Glass System.

AB Flux Zeropoints

Quantity	u	g	r	i	z	Notes and units
λ_{eff}	0.356	0.483	0.626	0.767	0.910	microns, from Fukugita et al. (1996)
$\Delta\lambda$	0.0463	0.0988	0.0955	0.1064	0.1248	microns, from Fukugita et al. (1996)
f_{ν}	3631	3631	3631	3.631	3631	Jy or $\times 10^{-23}$ erg cm ⁻² s ⁻¹ Hz ⁻¹
f_{λ}	859.5	466.9	278.0	185.2	131.5	$\times 10^{-11}$ erg cm ⁻² s ⁻¹ A ⁻¹ , calculated from above quantities
Φ_{λ}	1539.3	1134.6	875.4	714.5	602.2	photons cm ⁻² s ⁻¹ A ⁻¹ , calculated from above quantities

These are for the SDSS filters on the AB system. Data from Fukugita et al. (1996) repeat their Table 1, rows 1 and 6.

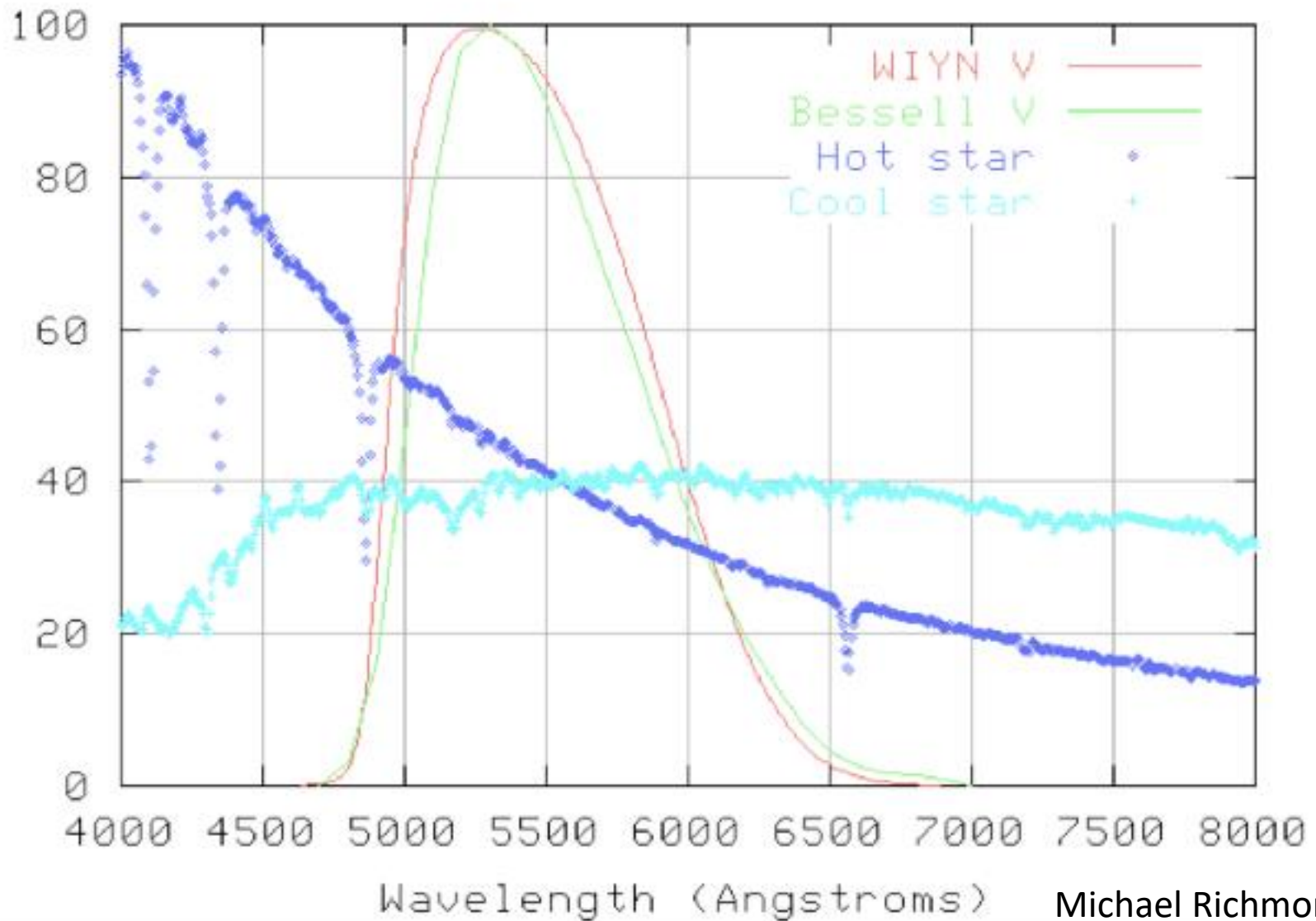
Note that the AB system is defined such that a source with $F_{\text{nu}} = 3.63 \times 10^{-20}$ erg cm⁻² s⁻¹ Hz⁻¹ has AB mag = 0 in every filter, and in general

From <http://www.astronomy.ohio-state.edu/~martini/usefuldata.html>

Filter bandwidth and Transformation

- Wide-band filters have significant colour effects.
 - e.g. in the visible a hot star has decreasing flux with wavelength, whereas it may increase in a cool star.
 - This means that the effective wavelength of the filter depends on the spectrum of the object measured.
- Filters with the same name are not identical
 - Different specifications and manufacturers lead to different bandwidths, transmission profiles
 - Transmission profiles are temperature dependent: they tend to narrow and shift to longer wavelength with decreasing T
 - Big differences can arise if strong, sharp spectral features are included in one passband, but not another
 - Instrument and atmospheric transmission also affects profile
- Need careful calibration to obtain accurate photometric measurements with different instruments

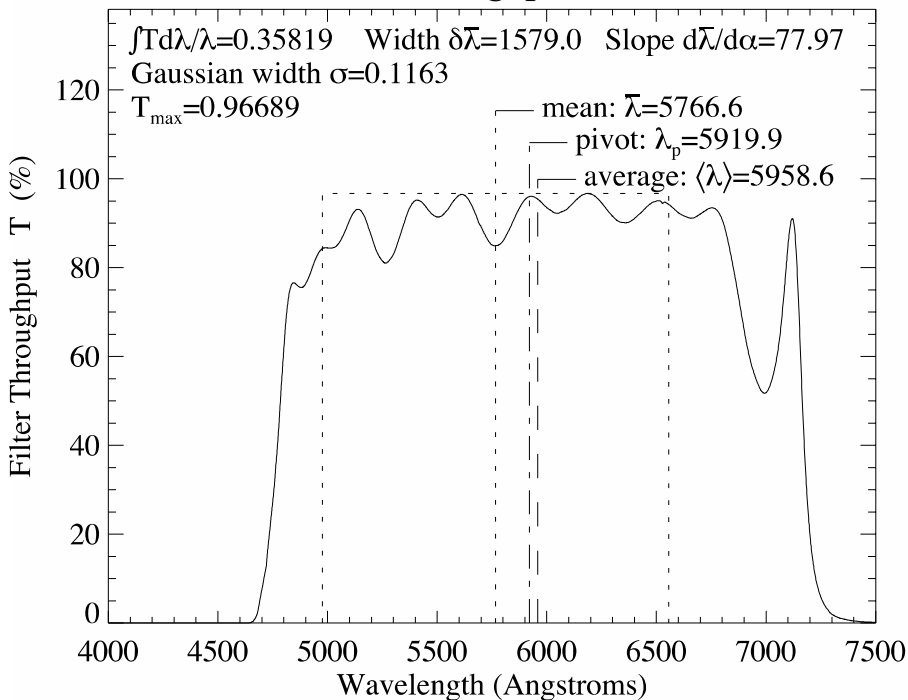
Filter Colour Terms



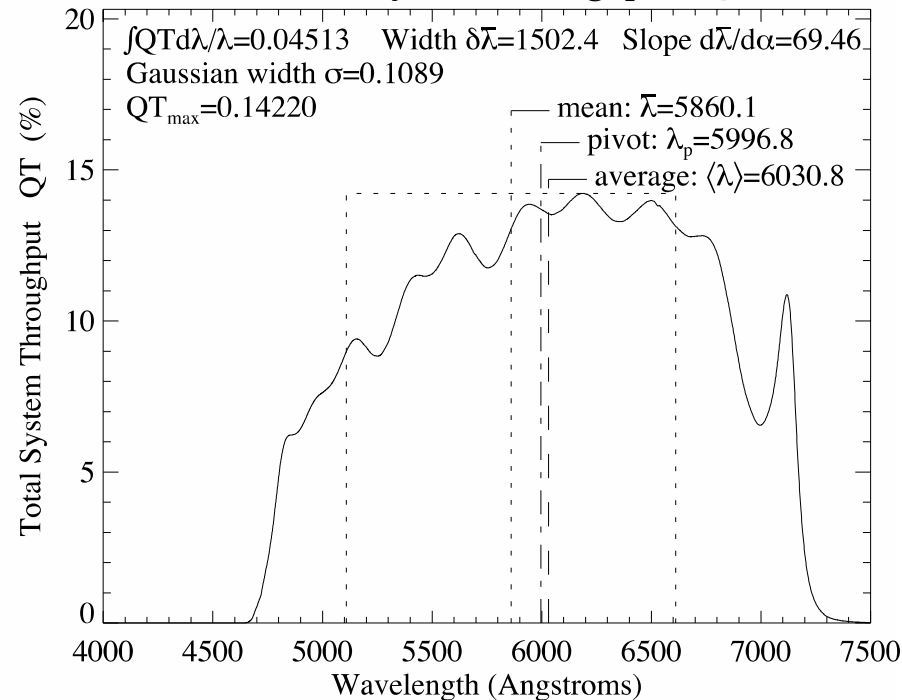
Effects of instrument/Detector Transmission

F606W (Wheel:10 Pos:2)

Filter Throughput T



Total System Throughput QT



Colour transformations have been derived in two ways: one empirically based on UFTI photometry and the other calculated by convolving the known filter profiles with spectroscopic data for a representative set of red stars. The two determinations agree well. The transformations between the old IRCAM3 system and the new MKO-NIR system at H and K are well behaved and single-valued. However, for the J filter different terms have to be applied depending whether or not the standard star has intrinsic water absorption features. This is due to the fact that the new J filter cuts off shorter than the old filter, specifically to avoid water absorption in the terrestrial atmosphere. For stars with no intrinsic water features the colour transformations are:

$$K_{\text{MKO}} = K_{\text{UKIRT}} - 0.020 [+/-0.005] (J-K)_{\text{UKIRT}}$$

$$(J-H)_{\text{MKO}} = 0.960 [+/-0.010] (J-H)_{\text{UKIRT}}$$

$$(H-K)_{\text{MKO}} = 1.205 [+/-0.010] (H-K)_{\text{UKIRT}}$$

$$(J-K)_{\text{MKO}} = 1.040 [+/-0.010] (J-K)_{\text{UKIRT}}$$

However, for stars with significant water absorption, stars with spectral type M4 through to the L class (but not including the T class with methane absorption):

$$K_{\text{MKO}} = K_{\text{UKIRT}} - 0.020 [+/-0.005] (J-K)_{\text{UKIRT}}$$

$$(J-H)_{\text{MKO}} = 0.870 [+/-0.010] (J-H)_{\text{UKIRT}}$$

$$(H-K)_{\text{MKO}} = 1.205 [+/-0.010] (H-K)_{\text{UKIRT}}$$

$$(J-K)_{\text{MKO}} = 0.980 [+/-0.010] (J-K)_{\text{UKIRT}}$$

The UFTI I- and Z-band filters are at significantly longer wavelengths than most optical CCD I and Z filters (with 50% transmission at 0.78 and 0.92 μm and 0.85 and 1.05 μm respectively). The I-band calibration has been compared to Landolt Cousins-I standards (Landolt 1992), and the Z system to the Sloan Sky Survey standards (Krisciunas et al. 1998). The Sloan Z values have been converted from an AB-system to our Vega=0mag system by subtracting 0.572mag from the Krisciunas et al. values. The following transformations were measured :

$$Z_{\text{UFTI}} = Z_{\text{S}} - 0.34 [+/-0.03] (I_{\text{C}} - Z_{\text{S}})$$

$$Z_{\text{UFTI}} = Z_{\text{S}} - 0.21 [+/-0.03] (Z_{\text{S}} - J_{\text{UKIRT}})$$

$$I_{\text{UFTI}} = I_{\text{C}} - 0.72 [+/-0.03] (I_{\text{C}} - Z_{\text{S}})$$

$$I_{\text{UFTI}} = I_{\text{C}} - 0.27 [+/-0.03] (I_{\text{C}} - J_{\text{UKIRT}})$$

The K-Correction

- Central wavelength shifts as a function of z
 - $\Delta\lambda/\lambda = (\lambda_{\text{obs}} - \lambda_{\text{em}})/\lambda_{\text{em}} = z$
- Bandpass stretches as a function of z
- Both effects accounted for in K correction
- No universal relation, related to intrinsic source spectrum
- See e.g. D.W. Hogg et al. 2002, astro-ph/0210394 for definitions and formulae
- Important factors to include when comparing objects at different redshifts – time dilation can also be important for transient events

From CCD frame to photometric data

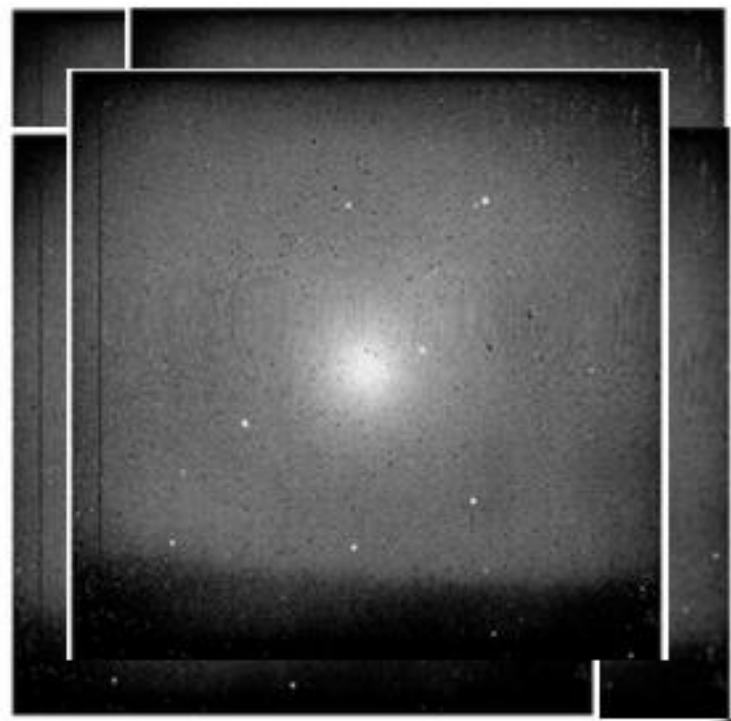
A properly sampled image will have least 2 pixels per FWHM (full width half maximum) of an unresolved stellar image. Note that some instruments undersample the seeing (e.g. VISTA) but then dither or drizzle by fractions of a pixel to improve sampling.

Before extraction of quantitative estimates of the signal, CCD frames must be **bias subtracted, dark count subtracted, corrected for non-linearity and flat field variations and cleaned of cosmic rays** (if necessary). The measured data values also need to be multiplied by the **gain factor** (the number of electrons per adu) to give the correct photon statistics

It is your responsibility to collect the correct frames for data reduction. Do not skimp even though it means you may have less time on-source. Check Data Reduction cookbooks & Instrument manuals

IR Data Reduction

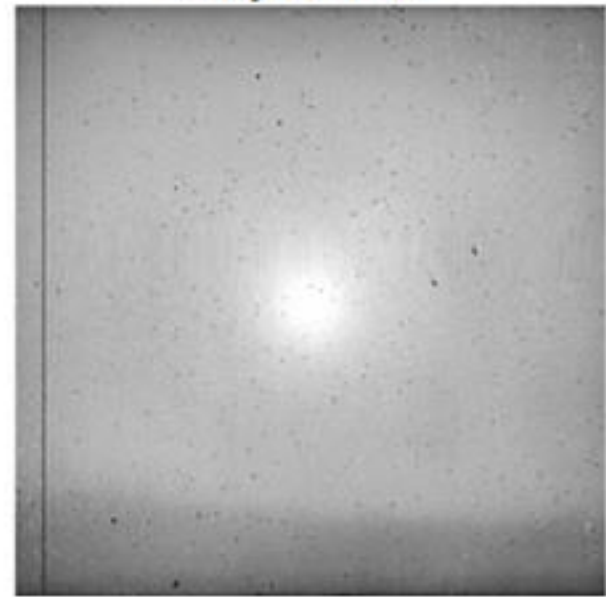
- IR array observations, need more attention to sky background, which is more variable and brighter than at shorter wavelengths
- Typically: obtain a median filtered sky flat from a sequence of images, that have been dithered around the field.
- Multiple observations of science field with small telescope motions in between (dithering) – short exposures are needed because of the bright sky
 - Note that this means that the final image will have a larger field than a the detector format, but that the edges will have less exposure and so greater noise.
- Sky subtraction before flat fielding minimises effects of flat field variations.



Median

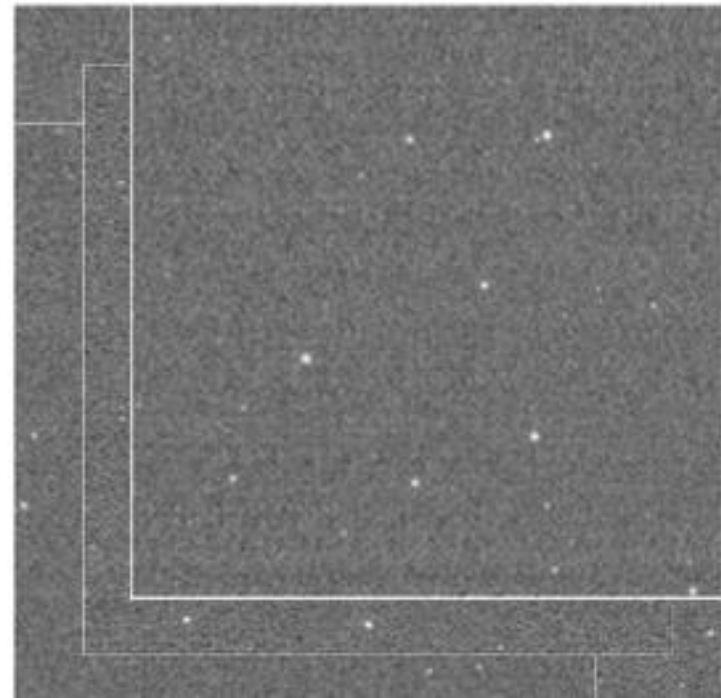


Sky frame



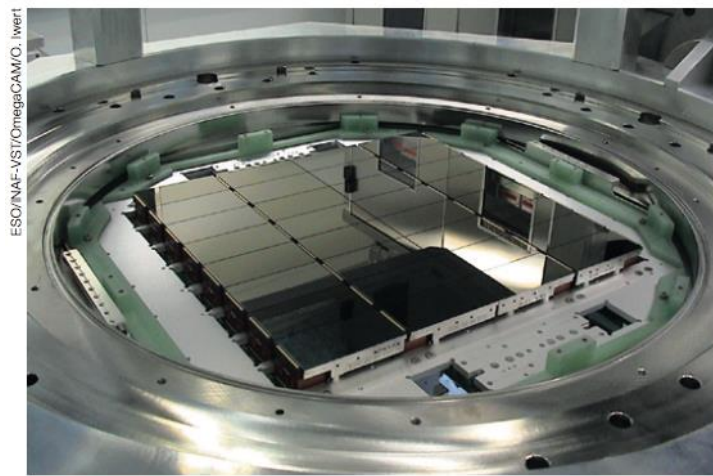
Subtract sky,
divide each by

Flatfield

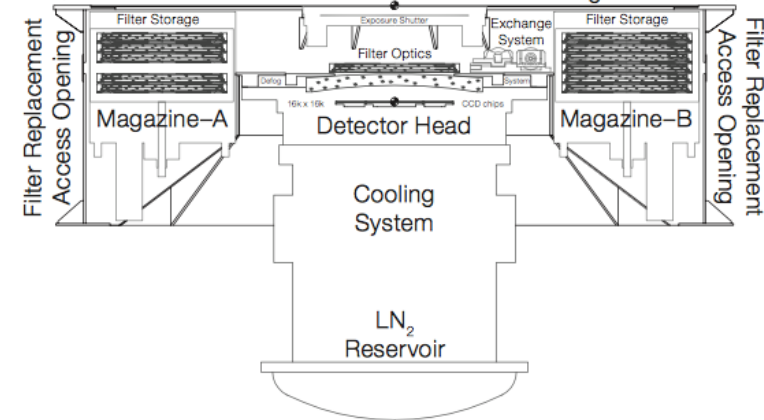


Cameras

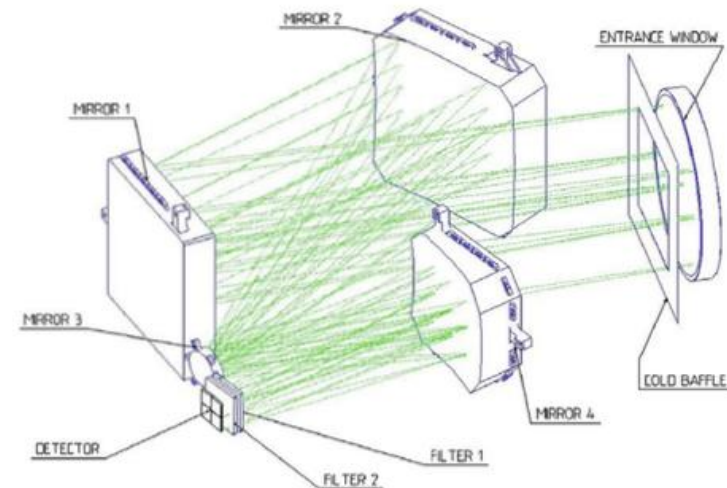
Visible wavelength imagers consist of (a mosaic of) detectors sitting behind a filter wheel in a cryogenic dewar. The 48 CCDs in the OmegaCam/VST camera are shown right.



Infrared instruments usually employ reimaging optics which produce an intermediate image of the telescope pupil to control the background, with the opportunity to deploy filters and other optical elements such as gratings or polarizing prisms near the pupil.



Bottom: the optical layout of the Hawk-I/VLT imager. It samples a 7.5' field at 0.1 arcsec/pixel with 4 x 2k Teledyne HgCdTe detectors. The mirrors image the secondary on to a cold pupil stop at M3 and convert the f/17.5 Nasmyth beam to f/4.4.

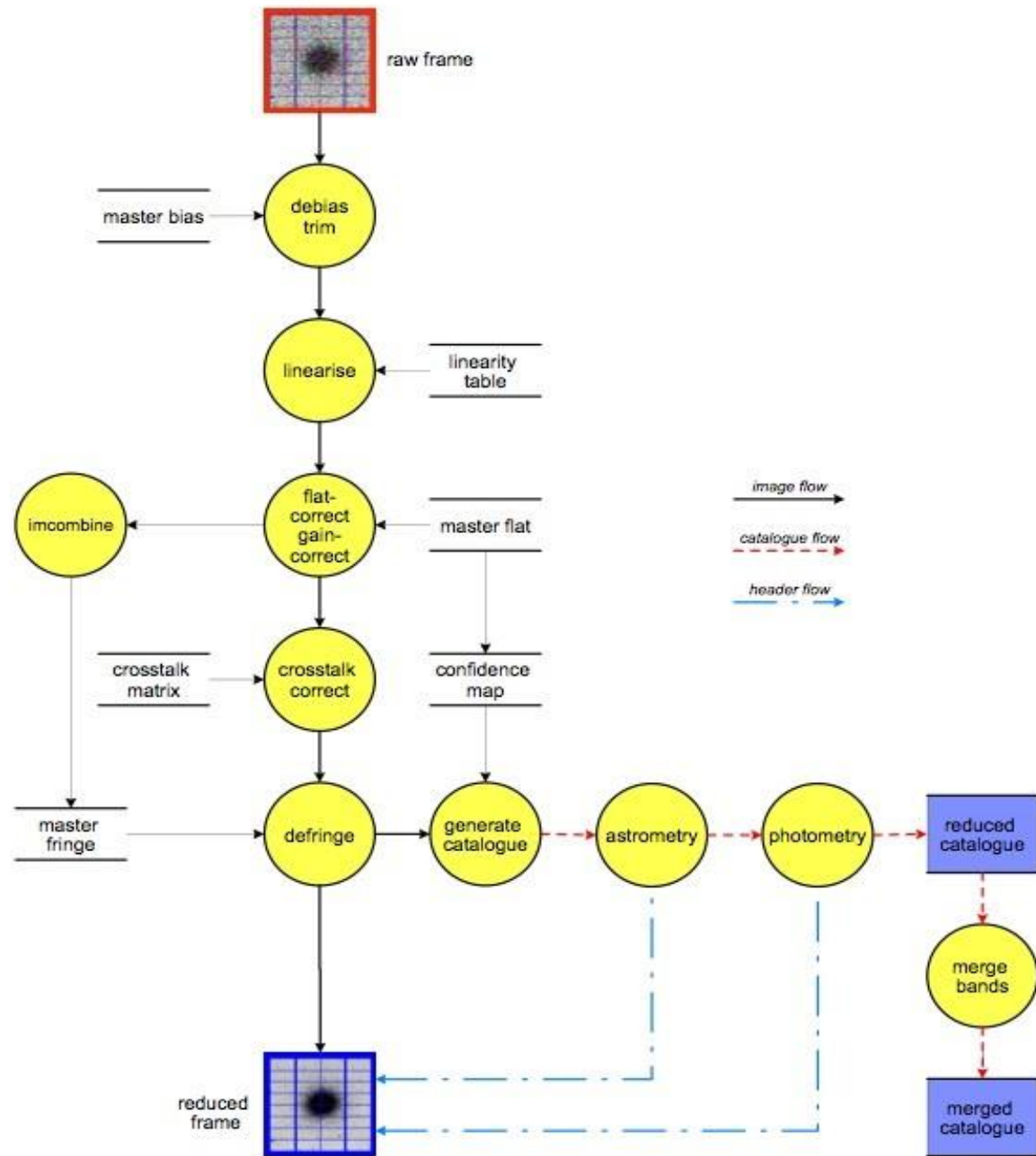


Multi-detector imagers

- Each detector will have its own characteristics - flat field, QE, dark current and operating pixel map etc.
- They will typically also be mounted in slightly different orientations and have different distortions – typically the images at the edge of the field will be more distorted than in the centre
- Accurate photometry or astrometry needs to take these into account
- Most observatories and reduction pipelines take these effects into account, but if you need particularly accurate values, (e.g. for lensing studies) you may need to re-reduce the data.
- Usually offer standard photometric filters + possibly special narrow-band filters for individual spectral features or to isolate emission lines at a particular wavelength.
 - In the IR, generally choose a bandpass between the atmospheric OH lines for lowest background and maximum sensitivity

Cambridge Astronomy Survey Unit

VST survey data
processing and
analysis flow chart



Thermal Backgrounds

At thermal infrared and sub-mm wavelengths, the background signal from emission from the sky and telescope on the ground is *much* bigger than the source, and much closer to the instrument

The background is time and position dependent and detectors may suffer from excess $1/f$ noise, so need to measure the background accurately and close in time to the target observations

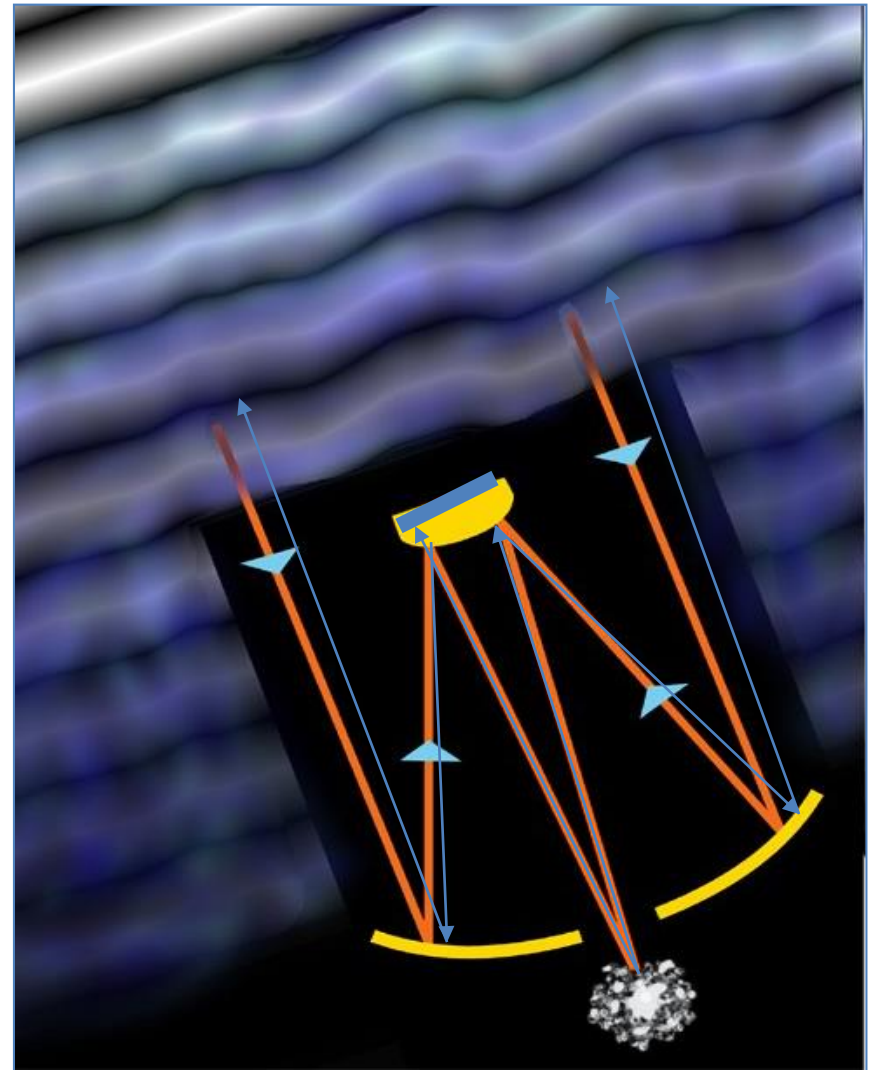
Generally employ chop-nod or rapid scan techniques to allow differential measurements between the target and the background

Space telescopes also have much lower but still variable backgrounds, but on longer timescales meaning chop-nod is not required. However, JWST data need background subtraction at long wavelengths

Chopping

- The telescope secondary mirror rocks in a quasi-square wave pattern at a few Hz, displacing the image of the object by ~ 20 arcsec on the detector. This allows the weak emission from the astronomical object to be detected differentially on top of the large thermal background
- The mirror position is stabilised with fast guiding at one or both chop positions, ideally chop in azimuth, but reduction will need to account for sky rotation
- Chop throw should be symmetric about the optical axis, and angles should be small so that image quality is maintained ; coma increases as angle increases
- BUT small throws mean that for extended objects, there may be residual flux in the reference position. For extended regions, reconstruction of chopped signals will be needed with consequent increases in observing time and complexity of data reduction and deterioration of S/N.

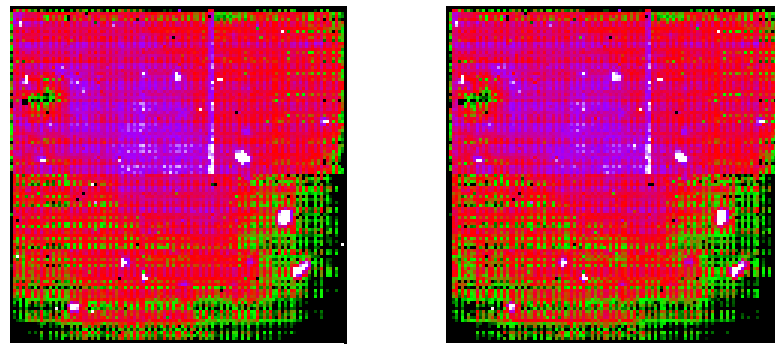
- Big telescopes are better for chopping as the beams separate higher in the atmosphere, and have more overlap on primary mirror
- But large telescopes have larger mirrors and so a greater moment of inertia.
- Focal plane choppers needed on the E-ELT
- E.g. Gemini: chop throw of 20 arcsec corresponds to $\sim 14\text{mm}$ in telescope focal plane
- and a motion of $\sim 11\text{mm}$ on the Primary of diameter of 7.9m
- Secondary mirror is undersized to ensure beam does not spill beyond the coated surface



Chopping and Nodding

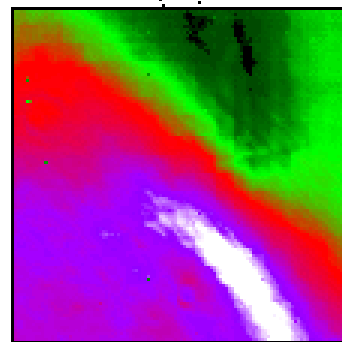
- Motion of secondary mirror, means that the detector beam falls on slightly different parts of the primary mirror, which have different defects, dust etc, leading to a radiative offset between the two chop positions.
- This is compensated by Nodding the telescope so that the object and reference positions are switched.
- Beamswitching :
 - Nod the telescope by a distance equal to the chop throw along the chop axis
- A-B gives net signal corrected for radiative offset
- BUT flexure and temperature changes mean that offset changes with time; observing sequence A,B,B,A removes linear gradient in offset.
- With beamswitching on-chip , final stacked frame has
 - one image with 2 x signal + 2 x sky background
 - two images with 1 x signal + 2 x sky background
 - Coadding all images gives an increase in S/N of $2/\sqrt{3}$ (30% in time)

Nod Position A



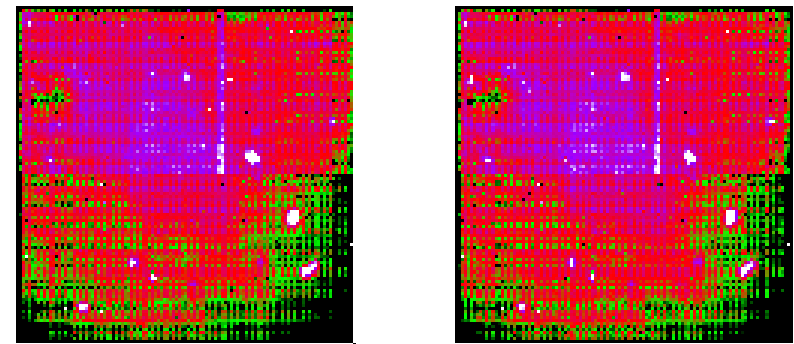
On-Source

Off-Source



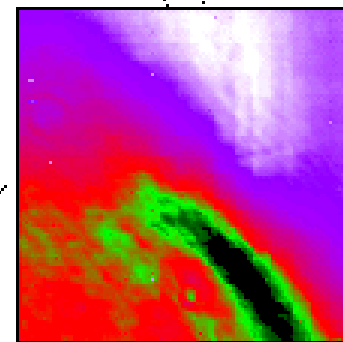
"Chopped Difference"

Nod Position B

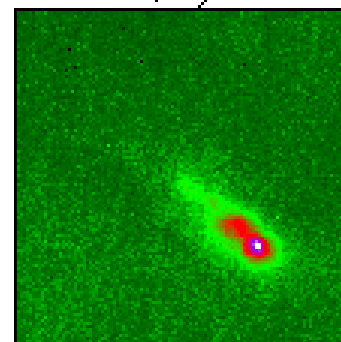


On-Source

Off-Source



"Chopped Difference"



Net Source Signal

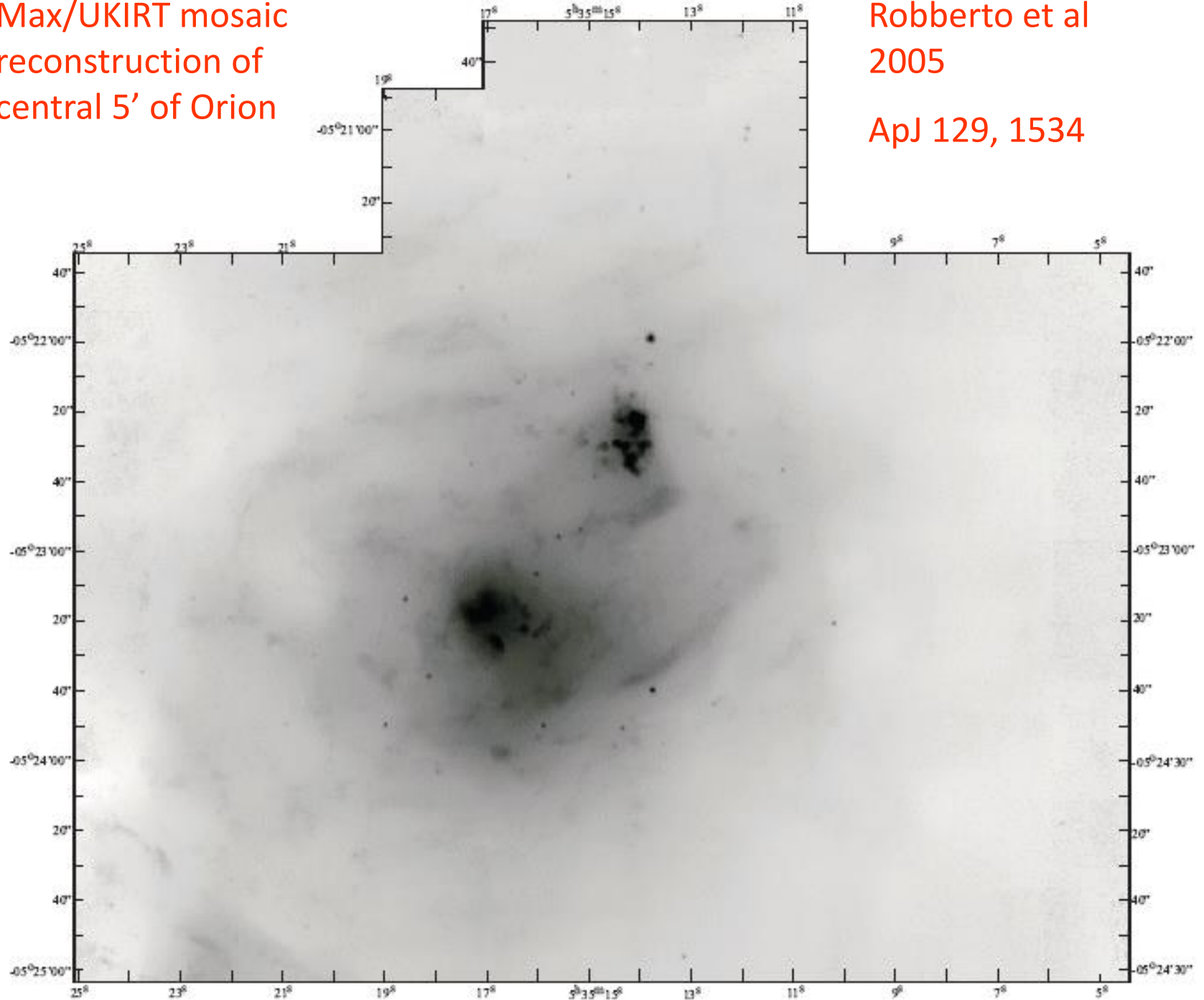
Sensitivity

- BLIP - Background Limited Performance
 - With backgrounds $>10^{10}$ photons/sec/ μm^2 , should get close to BLIP in all observing modes
 - Requires detector stability and performance, adequate filling of wells, efficient detector read schemes, low electrical noise
 - Theoretical Sensitivity depends on
 - Throughput of atmosphere, telescope & instrument
 - Detector QE (and noise sources - dark and read), read efficiency
 - Emission from sky, telescope and instrument window
 - Telescope efficiency, chop duty cycle, nod settle times, clocking efficiency

Max/UKIRT mosaic
reconstruction of
central 5' of Orion

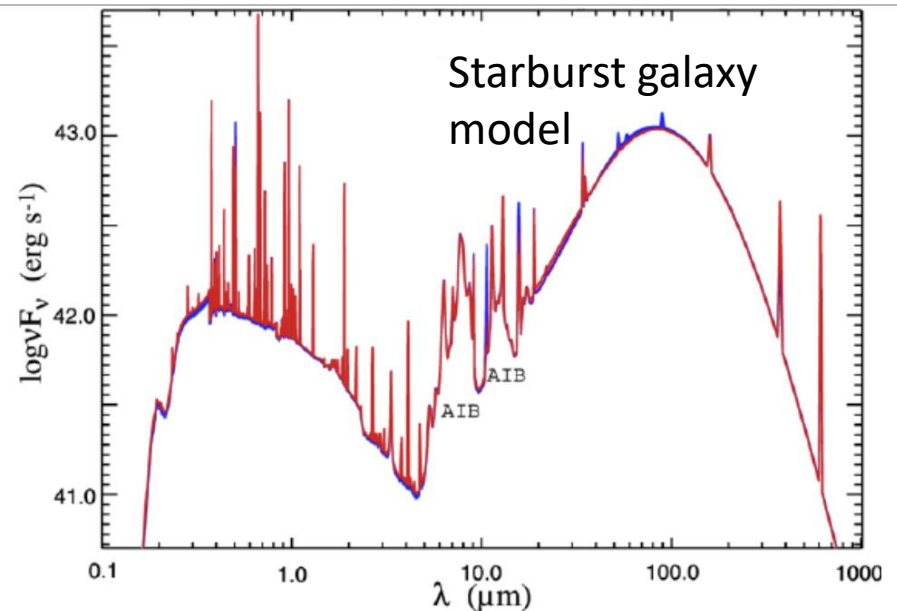
Robberto et al
2005

ApJ 129, 1534



Flux Density and other measures

- Definition of Jansky: $1 \text{ Jy} = 10^{-26} \text{ W m}^{-2} \text{ Hz}^{-1}$
- Radio Continuum normally given in Jy
- But lines may be expressed in K km s^{-1} or
- Antenna temperature
- Spectral energy distributions
in $\text{Wm}^{-2} = \lambda F(\lambda) = \nu S(\nu)$



Photometry with Interferometry

- Proceed cautiously!
- Fully processed – ‘Dirty’ - image has many residual structures which inhibit interpretation
- Generally CLEAN algorithm (Högbom 1974) is used to iteratively remove structure arising from the sample pattern in u,v plane of the brightest objects.
 - CLEAN needs intervention for extended objects and does not necessarily conserve flux
 - Can choose the resolution through deconvolution, but may not be sensitive to extended emission which can be distorted
 - Phase errors can redistribute signal within the image

<https://science.nrao.edu/science/meetings/presentation/jdf.webinar.4.pdf>

Interferometric Processing

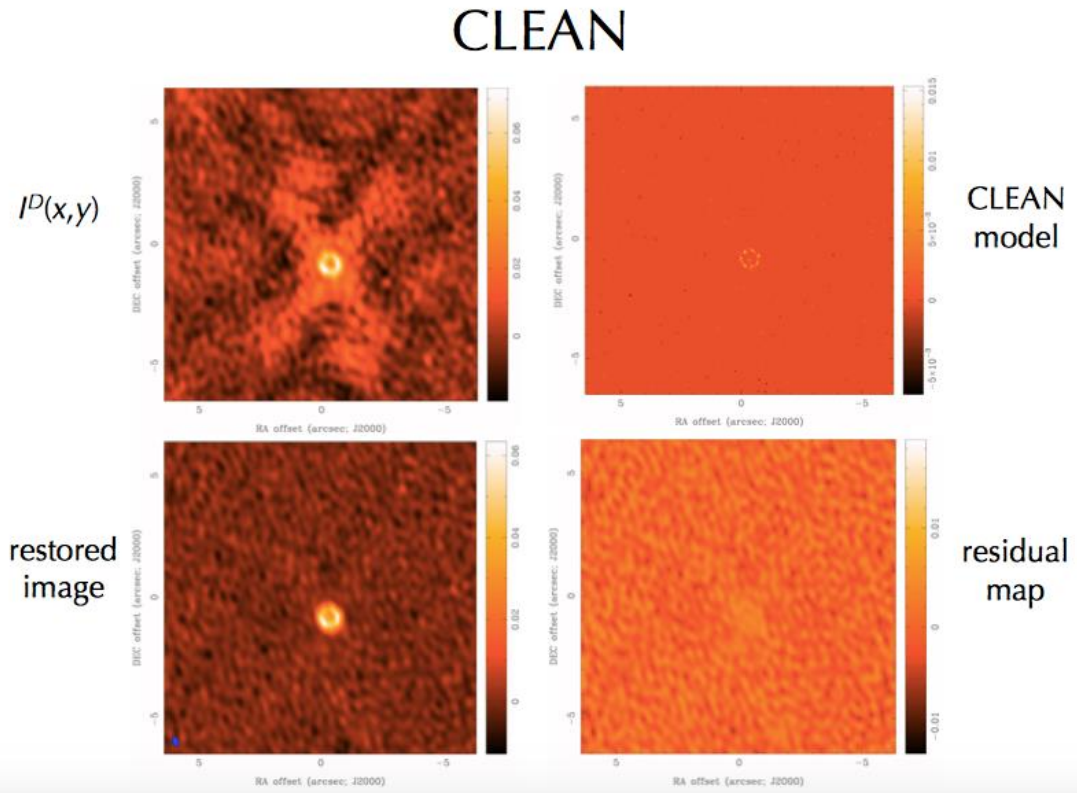
Measures of image quality:

Dynamic range

Fidelity - aliases

Signal-to-Noise ratio

Resolution



Space

In space, there is no need to compensate for the atmosphere!! The background is more stable, but is position dependent e.g. zodiacal light and thermal emission in the IR.

Diffraction-limited optics take full advantage of unaberrated wavefronts to yield exquisite, stable image quality and sensitivity

But still have detector characteristics to deal with: cosmic rays, variations in sensitivity across the field of view, changing thermal environments, and possibly image persistence if a bright object has been observed previously.

Radiation damage slowly increases the number of hot pixels and decreases the charge transfer efficiency in CCDs, so it is important to use up-to-date calibration data. There can be jumps in these properties after Coronal Mass ejections.

Coronagraphy

Coronagraphs can be used to suppress the light from bright stars or other compact objects.

These can simply be disks inserted into the focal plane, but more effective systems use a combination of focal and pupil plane masks to control the diffraction pattern.

Quadrant Phase Masks and other nulling systems may be effective, providing the telescope tracking is accurate.

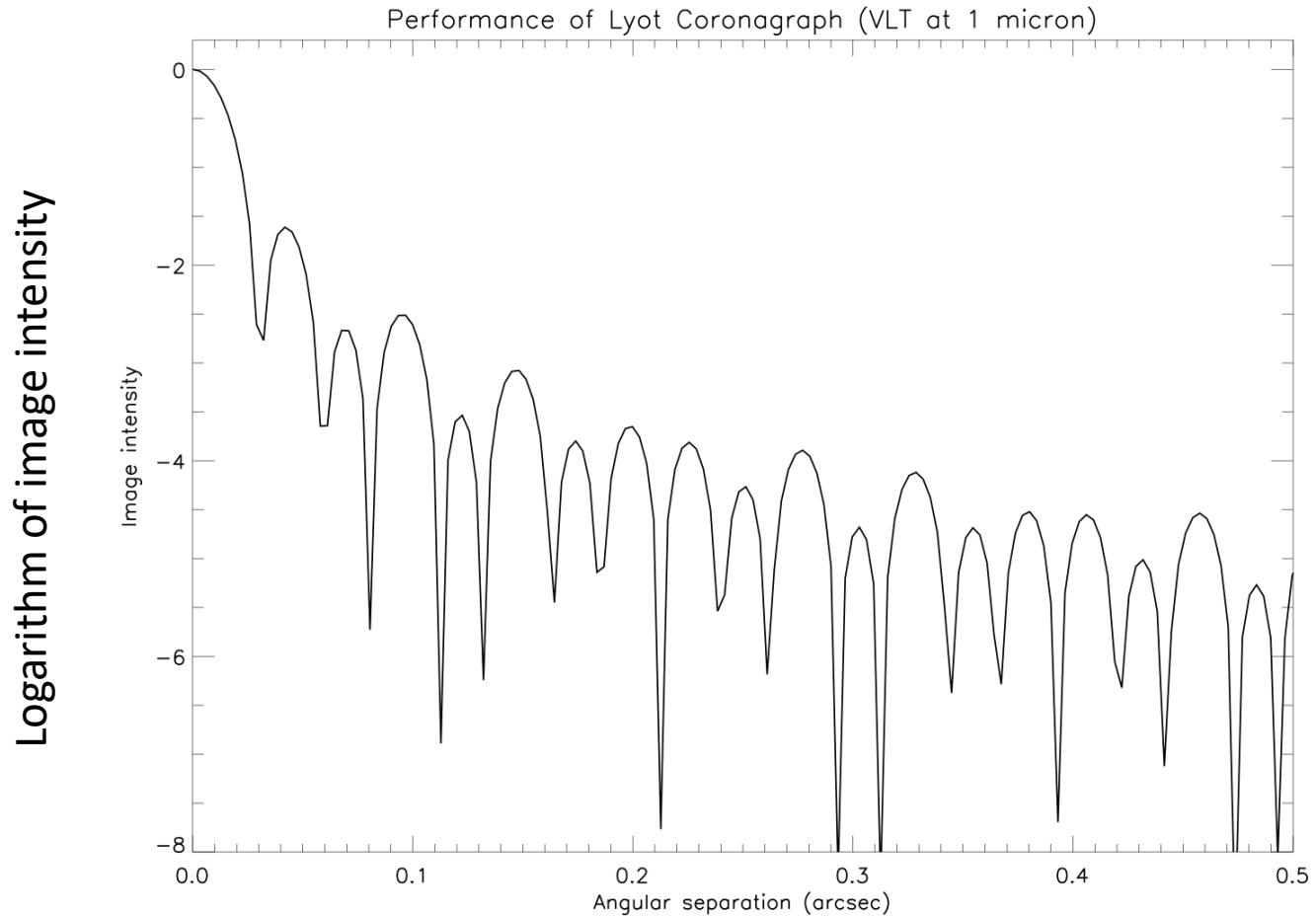
The SPHERE instrument on the VLT provides high-strehl AO, differential imaging, spectroscopy and polarimetry with coronagraphy for high contrast observations

The pale blue dot



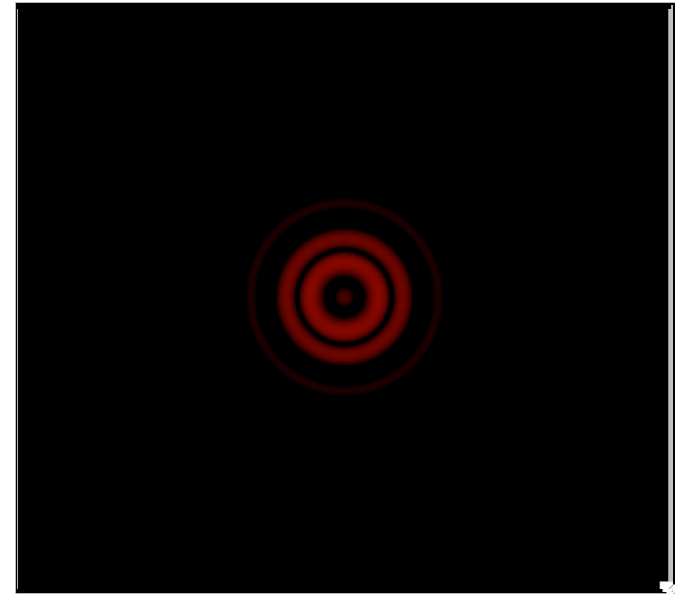
Picture taken by Voyager 1 probe looking back at the Sun from 40.5AU

Contrast curve with perfect Strehl

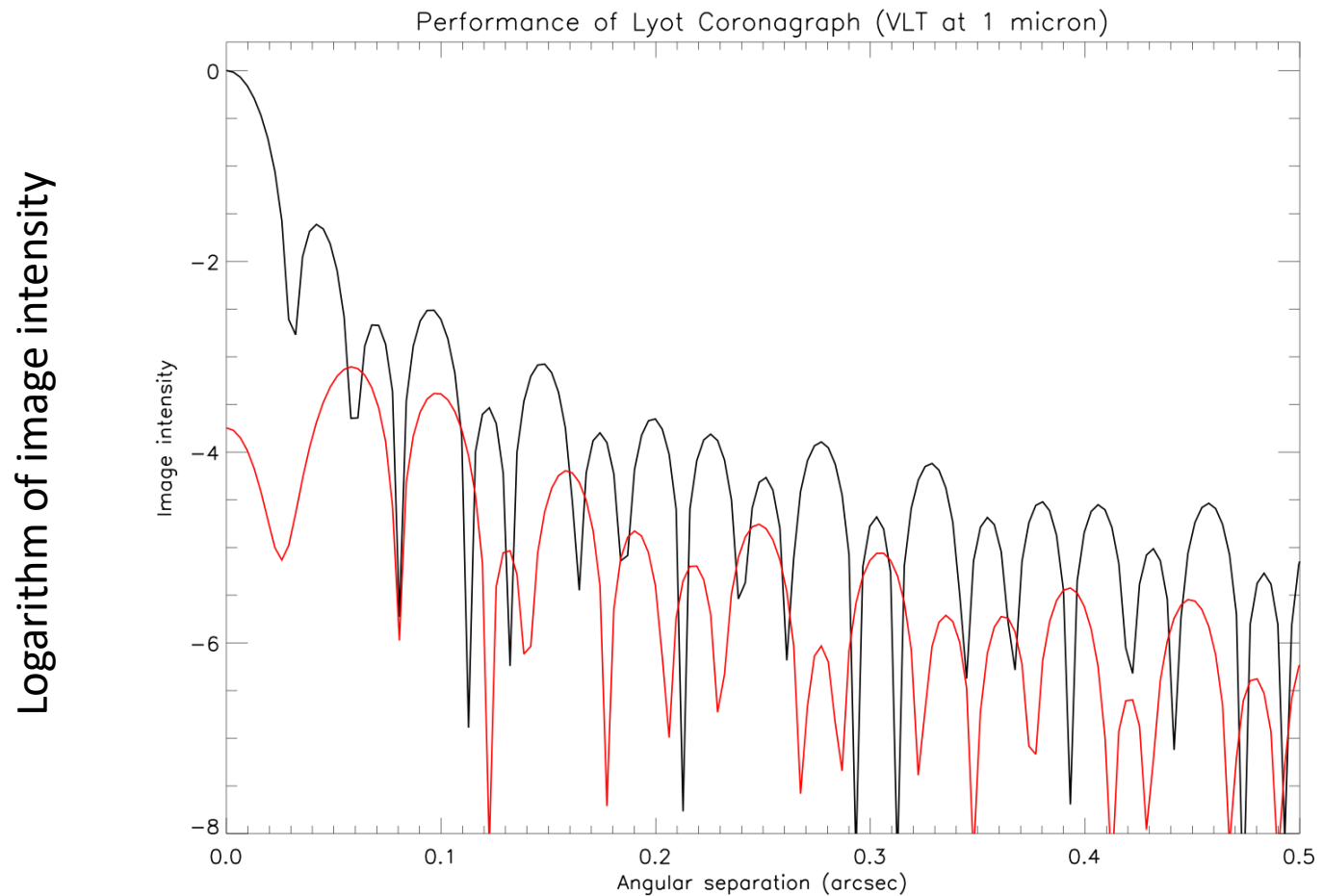


Coronagraphs

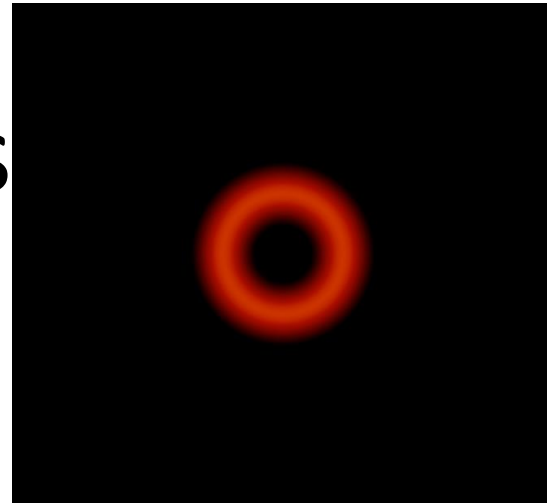
- Start with plane wavefront incident at telescope primary (pupil plane)
- Corresponding focal plane image is that of a perfect point source (Airy pattern with central obscuration)
- Introducing focal plane mask that blocks out peak of starlight
- Sharp edge leads to diffracted light at edges of pupil
- Lyot stop in pupil plane masks diffracted light
- Final image has much reduced intensity of starlight, planet unaffected except for small transmission loss.



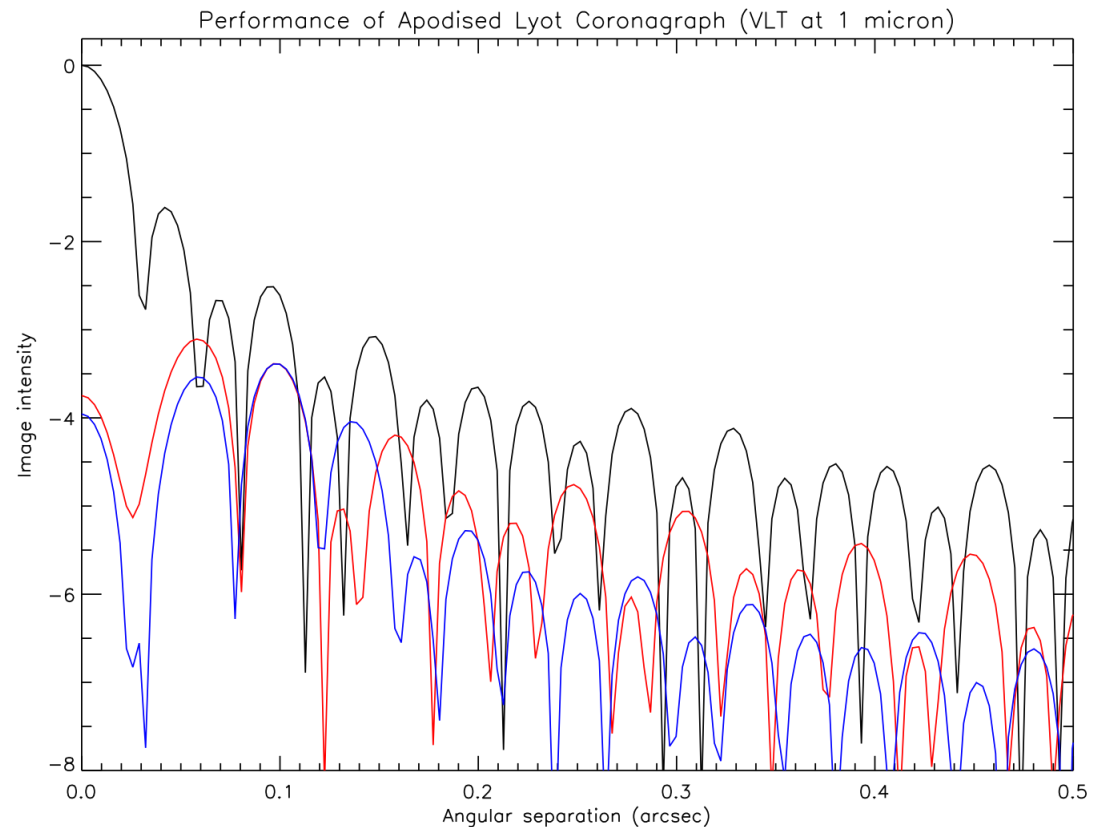
Contrast curve for Lyot coronagraph



Apodis



- Hard edges at pupil cause high spatial frequency “ripples”, which lead to lower contrast
- Solution: modify pupil plane distribution to remove all hard edges (Gaussian profile) - technique called apodisation
- Apodised Lyot coronagraph further improves achievable contrast.



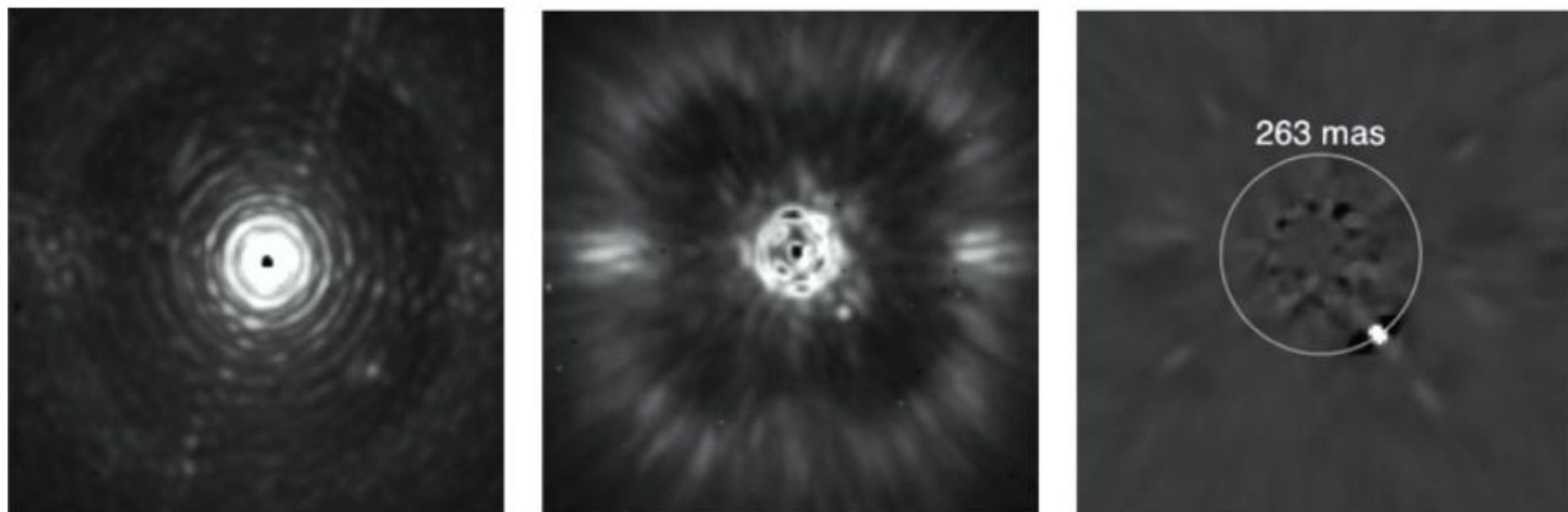
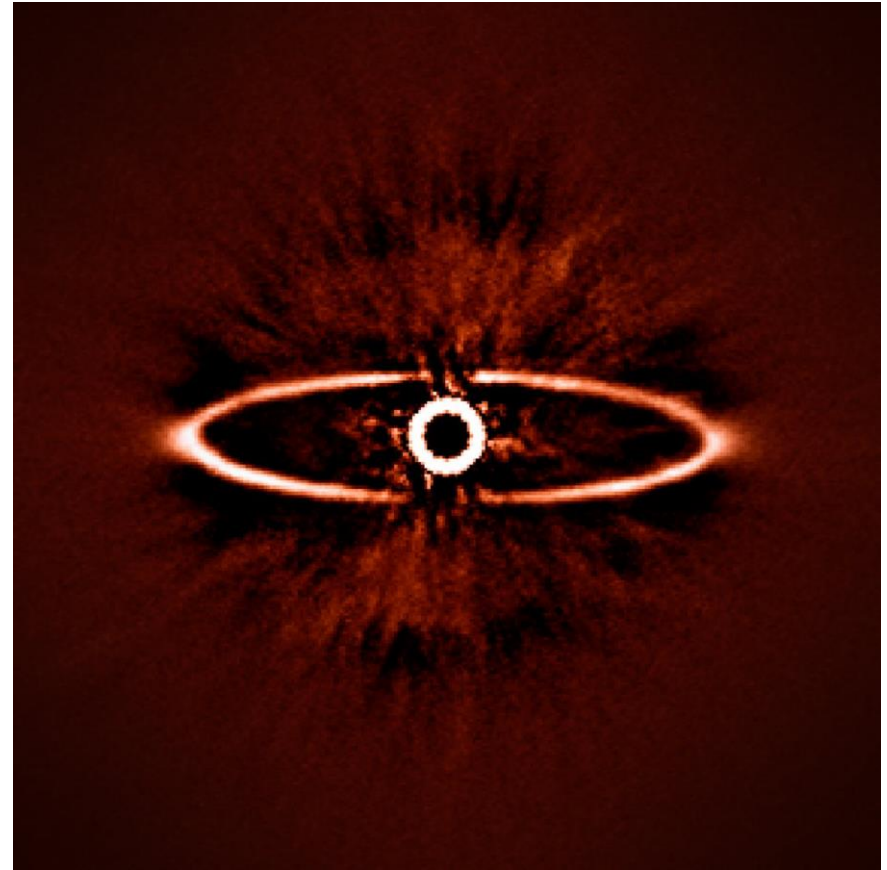
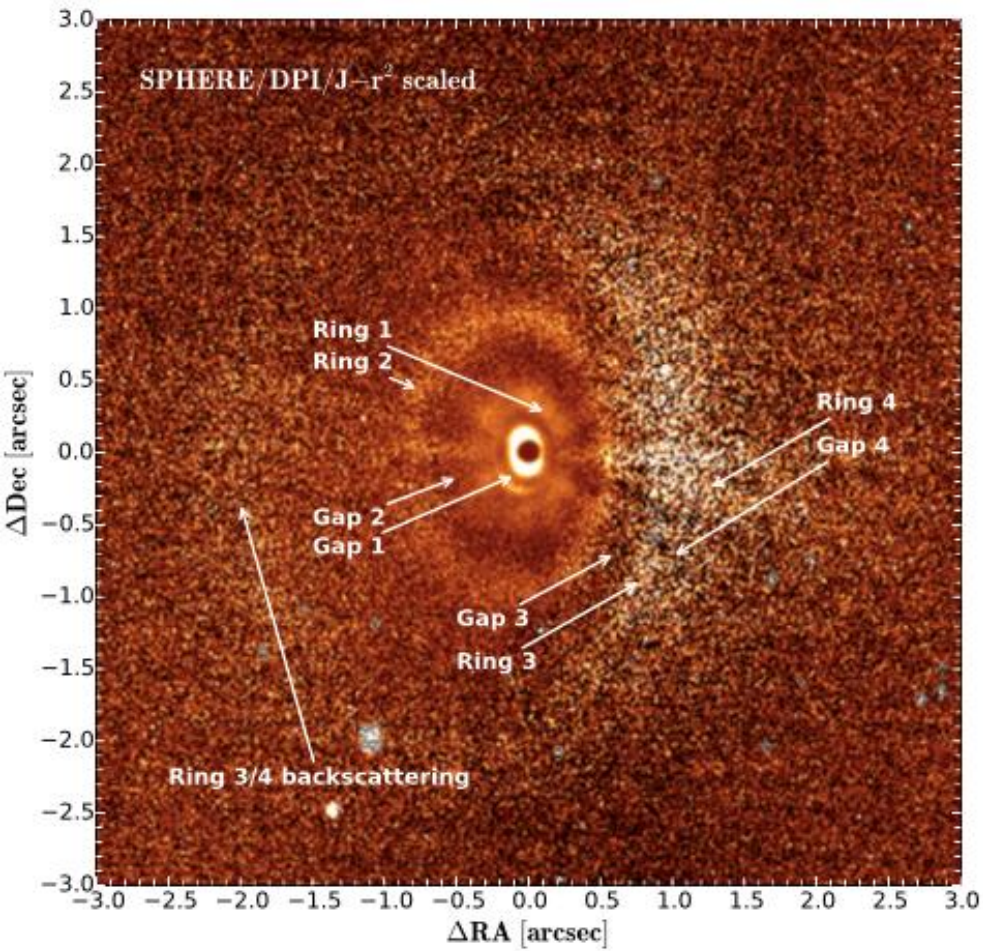


Figure 2: Illustration of the three pillars of high contrast imaging. Left: raw on-sky J-band PSF of SPHERE with IRDIS, showing the diffraction pattern resulting from the almost perfect correction provided by the extreme AO system up to $20 \lambda/D$ in the image (this figure is the number of actuator on the deformable mirror on a side divided by 2). Middle: raw on-sky J-band coronagraphic image of Iota Sgr, illustrating the efficient removal of diffraction rings and pinned speckles by the coronagraph. Note the very visible AO correction radius. Outside the correction radius ($r > 20 \lambda/D$), the brighter halo results from the uncorrected wings of the seeing halo. Right: result of angular differential imaging (ADI) strategy, and post-processing using principal component analysis, cleaning the remaining speckles in the field after extreme AO and coronagraphy, revealing a faint off-axis companion.



VLT/ Sphere images of HD97048 and HR 4796A

Space

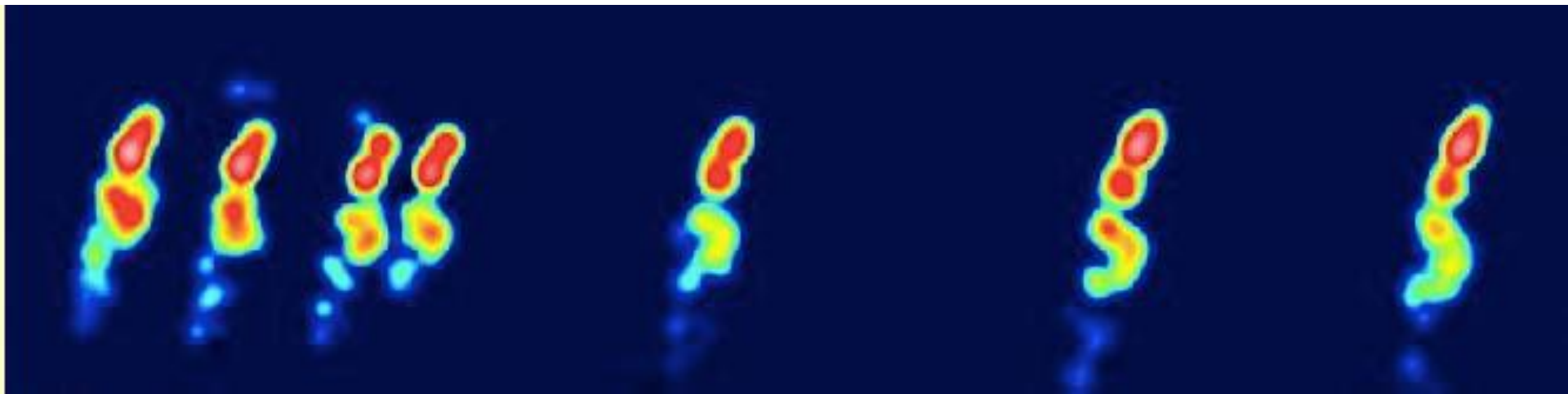
In space, there is no need to compensate for the atmosphere!!

Diffraction-limited optics take full advantage of unaberrated wavefronts to yield exquisite image quality and sensitivity

Interferometry in space can lead to higher resolution through longer baselines

e.g. VLBI using the HALCA satellite extended baselines to 30,000km at 5GHz

Note that the ISM is partially ionized and variations in refractive index can lead to dispersion, scattering and angular broadening at radio frequencies



Multi-epoch 5GHz images of the QSO 1928+738 between 1997 -2001 (DW Murphy)